TAMPEREEN TEKNILLINEN YLIOPISTO
TAMPERE UNIVERSITY OF TECHNOLOGY

KATARIINA TUOHIMÄKI

# ELECTROCARDIOGRAM AND IMPEDANCE PNEUMOGRAPHY MEASUREMENT MODULE DESIGN FOR TEXTILE-INTEGRATED SOLUTION

Master of Science Thesis

Examiners: Assoc. Prof. Matti Mäntysalo and Prof. Jari Viik
Examiners and topic approved by the Faculty Council of the Faculty of Computing and Electrical Engineering on 4th May 2016

# ABSTRACT

**KATARIINA TUOHIMÄKI**: Electrocardiogram and Impedance Pneumography Measurement Module Design for Textile-Integrated Solution
Tampere University of Technology
Master of Science Thesis, 52 pages, 1 Appendix page
July 2016
Master's Degree Programme in Electrical Engineering
Major: Biomedical instrumentation
Examiners: Assoc. Prof. Matti Mäntysalo, Prof. Jari Viik

Keywords: medical analog front-end, electrocardiogram, impedance pneumography, textile-integrated electronics

A wearable electronics is a quickly broadening category in sport, wellbeing and entertainment products. Also a fully textile-integrated electronics is used increasingly to improve the user experience. The medical industry is interested to exploit especially the latter technology for a supported long-term home care. The problem is, there are only wellbeing promoting textile-integrated electronics at the moment. These products recommend for example how to prevent an injury, but do not provide the actual diagnostic value. Purpose of this master´s thesis was to increase knowledge of the biomedical instrumentation about diagnostics textile-integrated electronics – especially designed for long-term home monitoring of the elderly.

For achieving this matter, into shirt integrated an electrocardiography (ECG) and impedance pneumography (IP) measurement module will be developed as a part of the Disappearing Sensors (DISSE) project. Preparation, like technical designing and functionality testing, have been made during this thesis for fulfilling described target. The functionality testing was implemented from three point of views: electrodes, measurement position, and measuring techniques for the ECG and IP. As electrodes were used commercial disposable electrodes, textile electrodes, and printed electrodes. Different measurement positions were laying, sitting, standing and walking slow and fast. As measurement techniques, 2- and 4-electrode measuring methods were compared by using commercial evaluation board. The work also considered a choose of the shirt and its final form in the prototype, which textile-integrated version will be completed during Autumn 2016.

From electrodes the most stable results were gathered with disposal ones. However, the skin irritation caused by these electrodes is not suitable for a long-term monitoring. For the textile and printed electrodes skin irritation did not seem to be a problem. Random instabilities of the textile electrodes were reason why the printed electrodes were chosen to be the best alternative. Measuring positions, excluding walking, fulfilled the minimum goal to detect pulse and breathing. In walking tests heart and respiration rates can be detected, despite occasional errors, only with disposal electrodes. In order to achieve the this with printed electrodes, the skin-electrode-contact should be improved. From two measuring techniques the 4-electrode measuring method had worse signal quality, but pulse and breathing were detected with more accuracy compared to 2-electrode measuring method.

# TIIVISTELMÄ

**KATARIINA TUOHIMÄKI**: Elektrokardiogrammia ja impedanssi pneumografia mittaavan moduulin suunnittelu tekstiili-integroituun sovellukseen
Tampereen teknillinen yliopisto
Diplomityö, 52 sivua, 1 liitesivu
Heinäkuu 2016
Sähkötekniikan koulutusohjelma
Pääaine: Biolääketieteen instrumentointi
Tarkastajat: Dos. Matti Mäntysalo, Prof. Jari Viik

Avainsanat: medical analog front-end, elektrokardiogrammi, impedanssi pneumografia, tekstiili-integroitu elektroniikka

Puettava elektroniikka on nopeasti kasvava ala urheilu-, hyvinvointi- ja viihdetuotteissa. Myös täysin tekstiiliin integroitua elektroniikkaa käytetään yhä useammin käyttömukavuuden lisäämiseksi. Lääketiede on kiinnostunut soveltamaan etenkin jälkimmäistä tekniikkaa tuetun kotihoidon pitkäaikaismonitoroinnissa. Ongelma kuitenkin on, että tällä hetkellä markkinoilla on vain hyvinvointia edistäviä tekstiiliin integroituja elektroniikkatuotteita. Näiden tarkoitus on esimerkiksi ehkäistä loukkaantumisia, mutta ne eivät tarjoa varsinaista diagnostista tietoa potilaasta. Tämän diplomityön tarkoituksena oli omalta osaltaan edistää lääketieteellisen tekniikan tieteenalaa kohti diagnostista tekstiili-integroitua elektroniikkaa etenkin vanhusten pitkäaikaisessa kotimonitoroinnissa.

Disappearing Sensors –projekti (DISSE) kehittää elektrokardiogrammia (EKG) sekä impedanssi pneumografia (IP) monitoroivaa mittausmoduulia, joka tullaan integroimaan kaupalliseen urheilupaitaan. Tavoitteen esivalmistelu, kuten moduulin tekninen suunnittelu ja toiminnallisuuden testaus, suoritettiin tämän diplomityön aikana. Toiminnallisuutta testattiin kolmella eri tavalla: elektrodeilla, mittausasennoilla sekä eri mittaustekniikoilla ECG:lle ja IP:lle. Mittauselektrodeina käytettiin kaupallisia kertakäyttöisiä elektrodeja, tekstiili-elektrodeja sekä kankaalle tulostettuja elektrodeja. Erilaisia mittausasentoja olivat makaaminen, istuminen, seisominen sekä kävely hitaasti ja nopeasti. Mittaustekniikoina vertailtiin kahden ja neljän elektrodin mittausmenetelmiä käyttäen kaupallista käyttöympäristöä. Työn aikana tutkittiin myös paitavaihtoehtoja sekä lopullista toteutusta tekstiili-integroidussa prototyypissä, joka valmistunee syksyn 2016 aikana.

Elektrodeista parhaimman tuloksen antoi kertakäyttöelektrodit. Toisaalta jatkuvan ihoärsytyksen takia niiden ei katsottu sopivan pitkäaikaiseen monitorointiin. Tekstiili- ja tuloste-elektrodien ei katsottu aiheuttavan iho-ongelmia. Tekstiilielektrodien vaihtelevan suorituskyvyn vuoksi, tulostetut elektrodit valittiin parhaimmaksi vaihtoehdoksi. Kaikissa mittausasennoissa, kävelyä lukuun ottamatta, voitiin havaita pulssi sekä hengitystaajuus, ja näin minimitavoite saavutettiin. Kävelytesteissä vain kertakäyttöelektrodit pystyivät satunnaisia häiriöitä lukuun ottamatta havaitsemaan sykkeen sekä hengitystaajuuden. Samaisen tulokset saavuttamiseksi tulostettujen elektrodien ihokontaktia tulisi parantaa, jos niitä aiotaan soveltaa tulevassa prototyypissä. Kahdesta mittaustekniikasta neljällä elektrodilla signaalin laatu oli huonompi, mutta pulssi ja hengitystaajuus havaittiin luotettavammin kahden elektrodin tekniikkaan verrattuna.

# PREFACE

This Master´s thesis was written for Department of Electronics and Communications Engineering at Tampere University of Technology. It was implemented as a part of Disappearing Sensors (DISSE) project, which is funded by Tekes (*the Finnish Funding Agency for Technology and Innovation; Disappearing sensors; rahoituspäätös 570/31/2015*), and co-operated with GE Healthcare, Clothing+, and Elisa.

I would like to thank my thesis examiners, Assoc. Prof. Matti Mäntysalo and Prof. Jari Viik, for the opportunity to be a part of this very interesting and futuristic project and for the valuable feedback during the work process. I would also like to thank everyone in the Laboratory for Future Electronics and DISSE project, especially B.Sc. Shadi Mahdiani for general ideas on measurement setups and support in data filtering. I would like to thank M.Sc. Javier Gracia and B.Sc. Vala Jeyhani for technical advices, and nurse Riina Kujanpää for professional input.

In addition, I would like to thank personnel of the Department of Electronics and Communications Engineering for this enjoyable working environment.

For M.Sc. Mikko Toivonen, my family and friends for all the support during the writing process of this thesis and my studies.

Tampere, 08.07.2016

Katariina Tuohimäki

# CONTENTS

# LIST OF FIGURES

# LIST OF SYMBOLS AND ABBREVIATIONS

| | |
|---|---|
| AC | Alternating current |
| ADC | Analog to digital converter |
| AFE | Analog front-end |
| AV | Atrioventricular |
| BIS | Bioimpedance spectroscopy |
| BLE | Bluetooth low energy |
| CM | Common mode |
| CMRR | Common mode rejection ratio |
| DC | Direct current |
| DNI | Do not install |
| DRDY | Data ready |
| ECG, EKG | Electrocardiogram |
| EIT | Electrical impedance tomography |
| EMG | Electromyogram |
| FDA | (American) food and drug administration |
| FIR | Finite impulse response |
| HR | Heart rate |
| ICG | Impedance cardiography |
| IIR | Infinite impulse response |
| INA | Instrumentation amplifier |
| IP | Impedance pneumography |
| LA | Left arm |
| LL | Left leg |
| PCB | Printed circuit board |
| PGA | Programmable gain amplifiers |
| QFN | Quad flat no-leads package |
| QFP | Quad flat package |
| RA | Right arm |
| RL | Right leg |
| RLD | Right leg driver |
| RR | Respiratory rate |
| SA | Sinoatrial |
| SPS | Sample per second |

| | |
|---|---|
| $\sigma$ | conductivity |
| $\rho$ | resistivity |
| A | surface area |
| $A_{CM}$ | amplified common mode voltage |
| $A_d$ | amplified differential voltage |
| AVDD | excitation signal voltage |
| AVSS | potential of returning excitation signal (analog ground) |
| C | capacitance |
| f | frequency |
| I | current |
| $\mathbf{J}_{LE}$ | lead field of the voltage measurement electrodes |
| $\mathbf{J}_{LI}$ | lead field of the current feeding electrodes |
| L | length |
| U | voltage |
| R | resistance |
| $R_{in}$ | internal resistance |
| $R_p$ | resistance of pull-up and pull-down resistors |
| S | sensitivity field |
| v | volume |
| $\Delta V$ | potential difference |
| $V_{CM}$ | common mode voltage |
| $V_d$ | differential voltage |
| $V_n$ | voltage in measurement point n |
| $V_{offset}$ | offset voltage |
| $V_{out}$ | voltage output |
| $X_C$ | reactance |
| Z | impedance |

# 1. INTRODUCTION

The number of aged people has been increasing in the human population. Due the progress, also chronic diseases are more common [1]. Medical technology has attempted to develop devices and solutions to answer this resources consuming issue. Purpose of this thesis is to introduce one modern solution, medical textile-integrated electronics, for easy long-term monitoring of the elderly.

Idea of the medical textile-integrated electronics is that the measurement device is a part of clothing, and there are no wires or external devices to limit mobility of the user. This is how the patient is allowed to live longer independently at home. The devices will alert help when measured vital signs change to be beyond the safety limits. Textile-integrated electronics can also enable remote diagnostic without meeting the patient or before the patient is reached in an emergency case. Medical care can be targeted at the right time, if state of the patient change worse. Despite of these potential benefits, there is still very few diagnostic textile-integrated electronics at the market. Demand exists and measuring method is widely socially approved at least in Finland, where over 60 % of the people would be willing to be tracked by the smart technology, in hypothetical case they being aged and living alone [2]. That is why the marketing share could be potential for the companies in medical instrumentation business.

Meaningful measurement parameters for aged patient are for example heart rate, respiratory rate, temperature and activity. Cardiovascular diseases are among the most common chronic diseases. The respiratory rate (RR) is an important indicator of worsening state of the patient´s health. Rising temperature is a common sign of an infection. Decreasing activity level might be a sign of disease progression. Activity level also clarifies whether the increased heart beat is caused by an illness or just by movements of the patient.

Disappearing Sensors (DISSE) project, at Tampere University of Technology, has begun to develop a smart shirt, which would measure pulse, breathing and activity of the patient in long term. The idea is to permanently integrate few battery-powered measurement modules to the textile. At the moment, already materialized modules for the project are microcontroller and Bluetooth low energy (BLE) including module and in this thesis designed module for the electrocardiography and bioimpedance monitoring. Future modules to be added are at least accelerometer for the activity monitoring. The ready prototype will finally be tested in real operational environment.

A goal of this thesis was design the textile-integrated electrocardiography (ECG) and impedance pneumography (IP) measurement module in schematic level for the DISSE project. Minimum goal was to detect respiratory rate (RR) and heart rate (HR) and extended goal was also to detect a full, diagnostic value offering, ECG signal. In addition, these measurements were preferred to be able to be gathered by using the 4-electrode measurement instead of the common 2-electrode measuring method.

For achieving these goals, the first thing was to find medical analog front-end, which are in medical measurement purposes designed precise analog-to-digital converter chips including main required electronics, suitable for the 4-electrode measurement method. Usually there is also commercial evaluation boards available for these chips. With the evaluation board of the chosen chip, ADS1292R from Texas Instruments, performance of the future measurement module was studied in demo level from three point of views: electrodes, measurement position, and measuring techniques. As recording electrodes were used commercial disposable electrodes, textile electrodes, and printed electrodes. Different measurement positions were laying, sitting, standing and walking slow and fast. As measurement techniques, two and four electrode measuring methods were compared by using commercial evaluation board. The work also considered a choose of the shirt and its final form in the prototype.

The most significant achievements in this thesis were to find suitable medical analog front-end, which allowed also the 4-electrode measurement method; to explain how the 4-electrode measurement method would indeed be a good or even better alternative compared to the common 2-electrode measurement method; to prove the printed electrodes to be limited but suitable solution for this kind of textile-integrated solution; and to show how and why measurement results variates during daily activities.

Figure 1 introduces the DISSE project in general and separated parts related to this thesis. Other visible parts are presented in grey. The project also includes other invisible parts like signal processing, data storing, and creating a user interface for data reading.

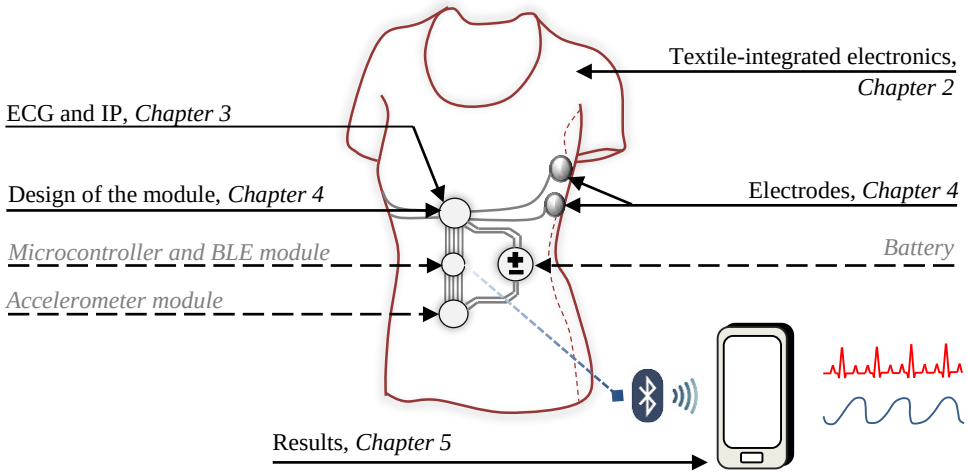


***Figure 1:*** *Parts of the DISSE project covered in this thesis.*

The chapter 2 of this thesis specifies wearable electronics and its subcategory, textile-integrated electronics. Also medical instrumentation point of view in both of these main and subcategory is covered. Chapter 3 explains measuring methods of the electrocardiogram and the bioimpedance in detail. Also diagnostic value of these two measurements is discussed. In chapter 4, design process and measurement plan of the thesis are presented. Chapter 5 contains the results corresponding to the previous chapter. Chapter 6 presents conclusions and future work for this thesis.

# 2. WEARABLE ELECTRONIC

During the recent years, wearable electronics have become more familiar for the customers. These products include commonly known heart rate monitors, fitness monitors, smart glasses, wearable cameras and music players, interactive T-shirts, movement sensing shoes, and USB hiding jewelry, as presented in Figure 2. It is predicted that by 2018, there will be 5.5 billion users only for mobile and wearable biometric technology [3].

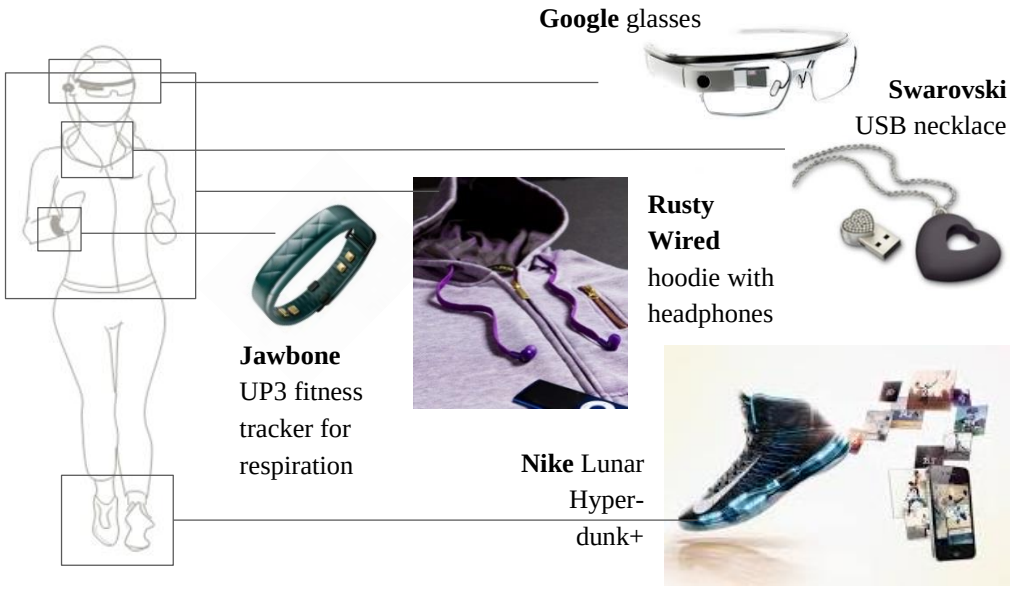


***Figure 2:*** *Commercial wearable electronics, adapted from [4–8].*

The wearable electronics may be used to produce safety for the user. For example, a Swedish safety company RECCO manufactures unobtrusive transmitters, which can send a signal to the rescue team in case of emergency, such as an avalanche. Hundreds of sport brands have decided to integrate RECCO products to winter sportswear, helmets and protection gear. [9] Nathan Sports pays attention to visibility of the runners and bikers. The company offers removable safety lights for shoes or alternatively for clothing and backpacks. [10] Tile has invented a small electronic device covered by plastic package. The device can be attached on keys, wallet, suitcase, bike, car etc., and can be located with a ringtone or a map application. [11] Many products have been designed to promote safety

and wellbeing of the elderly. For example Vivago`s wristwatch can alert help with integrated an alarm button, when needed [12].

## 2.1 Healthcare applications

Besides sports, welfare, entertainment and safety products, wearable electronics have also broadened possibilities to improve healthcare applications in totally new way. When the number of elderly people is growing in overall population, financial and resource related problems are increasing in healthcare industry. Especially for long term monitoring, staying supported at home is cost effective for the society and more comfortable for the patient.

The long term monitoring increases a possibility to discover abnormalities in vital signs. It enables anticipation and prevention of disorders. These are important elements in healthcare applications targeted to the elderly. Early state diagnoses and medication make difference on the prognosis of the patient and improves quality of life. For example, there is a possibility to slow down development of the memory disorders. [13] Because the monitoring takes place during everyday life, measurement device should able mobility of the patient. These ambulatory medical devices have established their position in medical instrumentation.

Maybe one of the most classical ambulatory medical devices is the hearing aid. An idea for improving the hearing started to develop already in the 17$^{th}$ century by using metal made ears. An acoustic horn was designed at the late 1800`s. The first electronically amplified hearing aids were offered by Siemens in 1913. [14] Ambulatory hearing aids may soon be replaced with implanted hearing systems, which were approved by the American Food and Drug Administration (FDA) in 2010 [15]. Other classical ambulatory medical devices, specifically designed for long term monitoring, are ambulatory electrocardiography, ambulatory electroencephalography, ambulatory oximeter and minimally invasive ambulatory insulin pump. The ambulatory electrocardiography is used to observe electrical activity of the heart over time. This measurement is described more closely in chapter 3. The ambulatory electroencephalography is similar to the electrocardiography, but it measures electrical activity of the brain. The ambulatory oximeter can be used to monitor the progression of lung diseases and impact of medication in long period of time. The half-invasive external ambulatory insulin infusion pump is good alternative for diabetics, who do not manage to achieve treatment balance, or for those who feel the insulin injection uncomfortable.

An example of a recently designed ambulatory device is the Triggerfish by Sensimed. It is a disposable contact lens embedding a micro-sensor that monitors continuous ocular changes over 24 hours. This product is designed to be used only at presence of healthcare professionals. [16]

## 2.2 Textile-integrated solutions

A textile-integrated solution is a subcategory of the wearable electronics, where electronics is included in clothing and cannot be removed. From the medical instrumentation point of view, the textile-integrated solutions are improvement from the ambulatory medical equipment. In the textile-integrated solution components are even lighter and more inconspicuous for others and for the user. When the product is a part of the user clothing, measurement device is more easy to remember to wear compared to the items such alarm buttons or pendants. The user is also external-wire free, which increases mobility.

Some medical devices require electrodes. When the electrodes are included in the textile, the user do not need help of the healthcare professional for precise placing of the sensors. The main advantage is a non-contact feature. With the textile-integrated electrodes it is possible to avoid skin irritation caused by commercial disposable electrodes, as seen in Figure 3. In the Figure 3 a. the most visible part of textile-integrated electrodes is the edge of the black laminated textile base. When observed closely, one can see also thin line caused by the lower textile-integrated electrode. Skin irritation from disposable electrodes, however, can be easily detected.

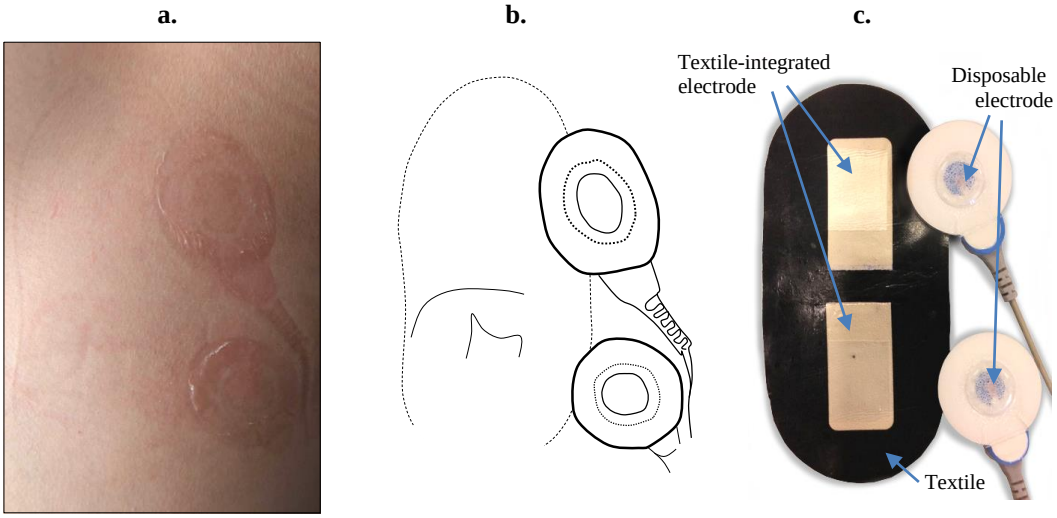


***Figure 3: a.*** *Skin irritation,* ***b.*** *visible marks on skin, and* ***c.*** *electrodes.*

Electrode equipped clothing has to be very fitting to guarantee good skin contact of the electrodes. This is achieved by using flexible fabrics. The material also has to be thick enough to enable applying of the textile electrodes and measurement modules. The third requirement is that electrodes should stay at the same place on the skin. It means electrodes should not move while the user is moving. For example, rising hands while wearing a shirt with sleeves can cause motion artefacts to the measurement signal. For elderly,

maintenance of the smart clothes can become a problem and should also be considered in design process [17].

Several textile-integrated prototypes have been developed for the medical purposes. Because there are not yet clear standards for implementing electronics to the textile, different solutions for electrodes and wires have been presented. For example, printed stretchable interconnections have been proposed for wiring [18]. Even though the printable wires could save resources in the manufacturing phase, sewn conductive wires are still more commonly used. Schlebusch et al. created a non-invasive bioimpedance spectroscopy (BIS) for long term monitoring of the lung edema. They decided to use polysiloxane electrodes and sewn textile wires. [19] Very similar technique was used in a wireless 12-lead ECG (*see chapter 3.1.2*) smart shirt designed by Morrison et al [20]. For the shirt were used commercial available electrodes by Polar USA. Seoane et al. [21] were interested to study how individuals experience and control stressful situations during the military service. In addition of the ECG and respiratory sensing shirt, they also designed gloves to measure galvanic skin response and body temperature, for evaluating a mental state of the user. Non-contact dry electrodes can also be based on magnetic field and induction current like in the magnetic induction (MAIN) shirt from Teichmann et al. [22], where litz wire was sewn into the textile as a shape of simply, one round coil. These kinds of electrodes were able to create injection current and measure obtained respiration and pulse.

The medical instruments are highly regulated and need often the professional user. That is why the most of the generally available textile-integrated wearable electronics are still targeted for wellbeing, sport and entertainment. While manufacturers cannot claim a product to be usable for the diagnostic purposes, they can provide recommendation for the user. A good example is in 2014 International CES Innovations Design and Engineering awarded Reebok Checklight. Purpose of this product is to prevent the user from training too hard or too quick after the head trauma [23]. MBODY from Myontec is electromyography monitoring shorts. It guides how to optimize a warm-up time and to detect imbalance in the muscles. In addition, the MBODY replace common heart rate monitors in many ways [24]. OM Smart Shirt is also bypassing usage of the sport watch and the heart rate belt. All similar elements are included to the textile, and a light removable smart box transfers information to the mobile application [25]. For those, who still prefer common heart rate monitors, Suunto and Salomon offers more comfortable replacement for the belt. In the Movesense product, heart rate sensor is integrated directly into the sport bra or the T-shirt [26].

The textile-integrated electronics gives also surprising possibilities for the entertainment business. WE:EX has developed totally new kind of smart T-shirt targeted for players and especially fans of the American football. Team members are wearing T-shirt which measure bio-signals like heart beat and pressure caused by contacts. Fan´s T-shirt is repeating sensing of the selected player [27]. Ideas like these might someday to be conducted to the

wellbeing and even the medical solutions. In the future, our clothes might give us physical feedback to watch out for a car or warm and cool down the one´s body according the ambient temperature.

In Figure 4 is listed overview of all products and prototypes introduced in this chapter. The figure also clarifies relation between wearable electronics, ambulatory devices and textile-integrated electronics.

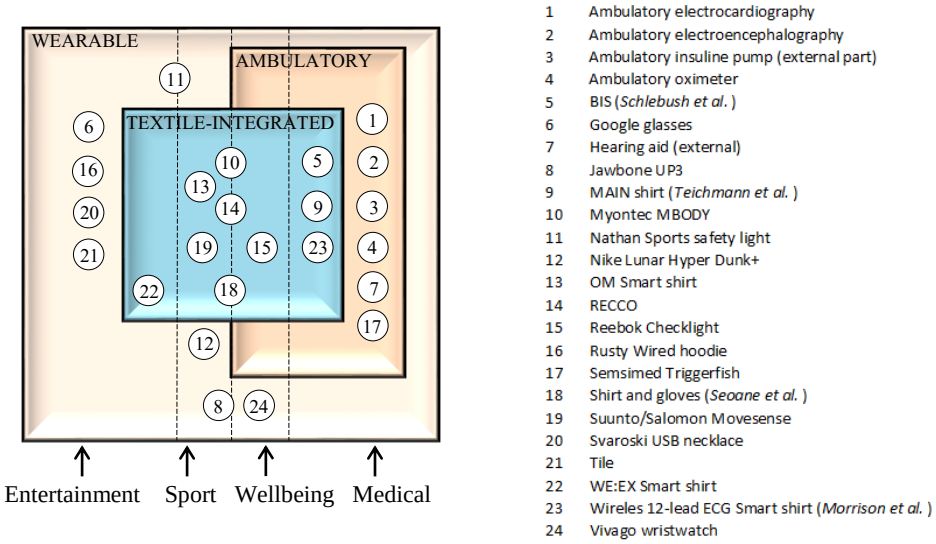


***Figure 4:*** *Categorized summary of the products and prototypes introduced in the chapter 2.*

The target area of this thesis is placed on medical textile-integrated solutions, where prototypes number 5, 9, 23 are presented. This target area was also heavily directing which kind of product were gathered to this chapter. Hence, Figure 4 does not show correct distribution between categories of implementation or purpose of use. For example, it would be relatively easy to list many other products to wearable electronics for entertainment, sport and wellbeing purposes.

# 3. PRINCIPLES OF ELECTROCARDIOGRAPHY AND IMPEDANCE PNEUMOGRAPHY

Healthcare professional consider heart rate (HR) and respiration rate (RR) to be primary physical quantities for long-term monitoring of elderly [28]. When either rate is beyond the normal limits, it can be seen as an indicator of the disorder in the body. Other important quantities to be monitored are acceleration and temperature.

In this thesis it was focused to make a design for measurement module, which could detect HR and RR. At least the accelerometer module will also be implemented into the ready prototype. The HR can be measured by using an electrocardiography, which produces an electrocardiogram (ECG) signal. In addition, the ECG gives information about electrical behavior of the heart. The specific bioimpedance method, impedance pneumography (IP), is used to gather information about the RR. Normally the RR is determined to be number of breaths per minute.

The ECG and RR are important parameters to be measured for the elderly. According to different studies in Europa and U.S., ca. 60 % of the elderly ($\geq 65-70$ years) have at least two chronic diseases [29–32]. In U.S., the forecast is that number of people with choric disease will increase with 50 % from 2010 to 2040 [1]. For example heart diseases, heart failure or cardiovascular diseases were listed among top five the most common chronic conditions in older age [1, 29, 30].

## 3.1 Electrocardiography

The heart is a critical organ. It serves as a pump for blood to flow through the tissues. Because of this transport system of the body is so important the heart is believed to be the first organ to become functional during development of a fetus [33].

Contraction of the heart, pumping, is caused by spontaneous electrical stimulus in autorhythmic cells (1 %) and contraction of contractile cells (99 % of the heart muscle) [33]. This electrical behavior is caused by the action potential of the cells, which includes depolarization and repolarization phases. In rest, the cells are negatively charged and extracellular liquid is positively charged. When action potential starts (depolarization phase), chemical and electrical balances between intra- and extracellular liquids are changed. Now sodium and calcium ions flow into the cell. At the same time potassium ions flow out the cell causing positive charge to the cell, and charge of the extracellular liquid change to negative. Action potential of the cell is quickly spread to the other heart cells via precise gap junctions. The action potentials, though, differs between autorhythmic (slow action potential) and contractile cells (fast action potential). [34] Besides of the

contractile cells, the small autorhythmic cells do not have a resting potential. The autorhythmic cells either do not contract, and they also prevent tetanus of the contractile cells. This refractory period occurs immediately after the repolarization and prevents another action potential to be generated at a certain time. [33] In Figure 5, the graph shows how the membrane charge of the autorhythmic cells eventually drifts towards the threshold. This phase is also known as a prepotential or pacemaker potential. When the threshold is achieved, a new action potential starts. Action potential of the autorhythmic cells stimulates the contractile cells. This is seen as a delay between two action potential signals. Because of the various sizes, ionic and conductivity behavior of the autorhythmic and contractile cells are different. Also shapes of the action potentials differ. [34]

The left side of Figure 5 presents overall conduction system of the heart. A heartbeat or more specific, the cardiac cycle, begins from the autorhythmic cells in the sinoatrial (SA) node. From the SA node it conducts to the atrioventricular (AV) node through conducting cells in intermodal pathways. Activated contractile cells make the atria to contract and blood flows into the right and left ventricles. Because the nodal cells are smaller in diameter than the conducting cells, an impulse slows down while passing through the AV node. This enables the atria contract before the ventricles do. From the AV nodal, the impulse conducts to the left and right bundle branches. Finally, the impulse reaches Purkinje fiber cells, which due their large diameter conduct action potentials very quickly. In this way, contraction of the ventricles proceeds from apex of the heart toward the base, and blood in the ventricles is pushed into the aorta and pulmonary trunk. [35]

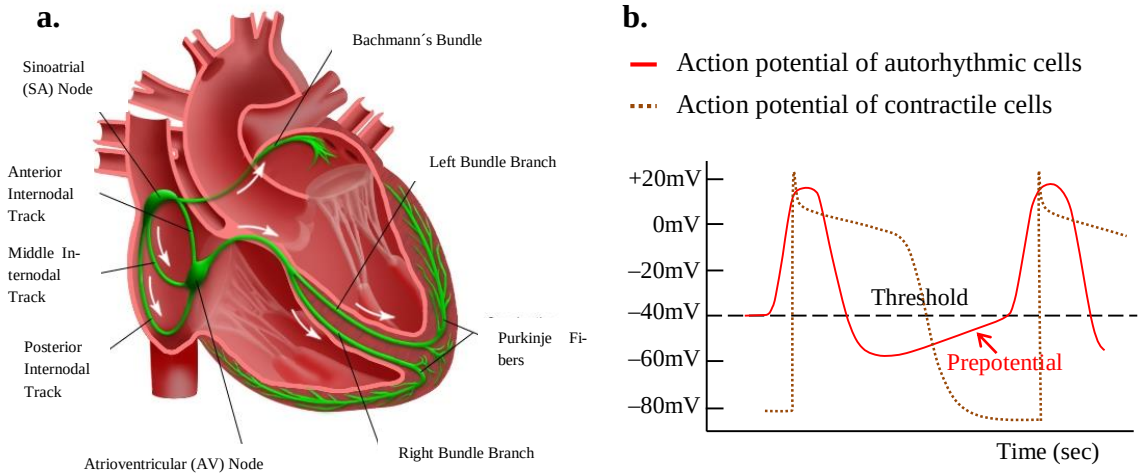


***Figure 5:*** *a. The conduction system [36], b. The action potentials, adapted from [34].*

A small part of electrical current, generated by cardiac muscle, is conducted on the surface of the body via tissue fluids. The potential differences can be detected by suitable at least

2-electrode measurement system. A recording of this activity is the ECG and a measurement procedure is the electrocardiography. [33]

Pattern of the ECG, measured from the body surface, is represented in Figure 6. The ECG, at the certain moment, is a sum of the action potentials in the cardiac muscle cells. Some the cells are activated while others are at the rest or prepotential states. Morphology of the signal depends on which part of the conduction system of the heart is active at the moment. In highlighted window of Figure 6, phases of the ECG are named. The small P wave is generated due depolarization of the atria. Actual contraction of the atria cells begins about 25 milliseconds after start of the P wave. Depolarization of the ventricles is called the QRS complex, which holds relatively strong potential. This is because the ventricles have bigger muscular mass compared to the atria. Contraction of the ventricle cells begins shortly after the peak of the R wave. Repolarization of the atria is masked by the QRS complex. Repolarization of the ventricles is shown as the T wave. [35]

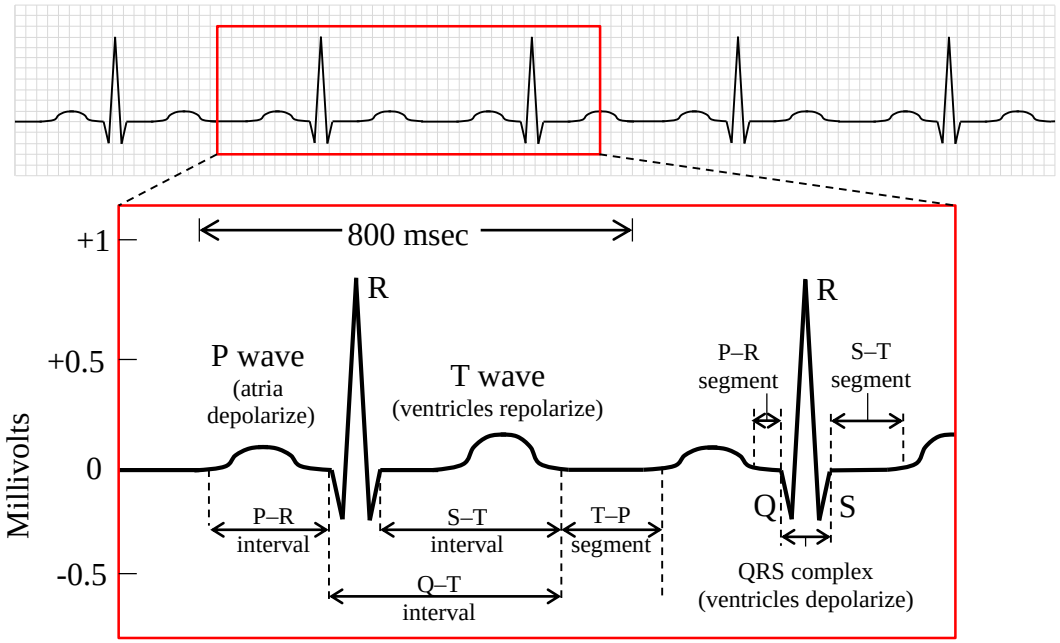


***Figure 6:*** *Segments and intervals in ECG printout, adapted from [35].*

There are three phases between waves where no current is flowing in the heart tissue and the ECG remains at the baseline. These parts are segments. The P–R segment is caused by the delay in the AV node. Magnitude of this signal is too small to be detected in the ECG. The S–T segment represents time when ventricles are completely contracted and emptying from blood. Before a new cardiac cycle, there is the T–P segment, in which the heart muscle is resting and the ventricles are filled by blood. [33] Intervals are more variable than segments, but they always include at least one entire wave [35]. Intervals offer diagnostic information about the ECG and are discussed in chapter 3.1.2.

### 3.1.1 Standard 12-lead electrocardiography

The ECG can be measured as a potential difference from two different points on the body surface. A simply equation can be presented as,

$$\Delta V(t) = V_2(t) - V_1(t), \quad (1)$$

where ΔV is the potential difference, $V_1$ is the voltage in the first measurement point, and $V_2$ is the voltage in the second measurement point. These voltage changes were first measured by a medical doctor and physiologist Augustus D. Waller in the end of the 1800 century [37] [38]. Figure 7 shows an early ECG, which is measured from front and back of the chest. At that time, this measurement was called a cardiograph.

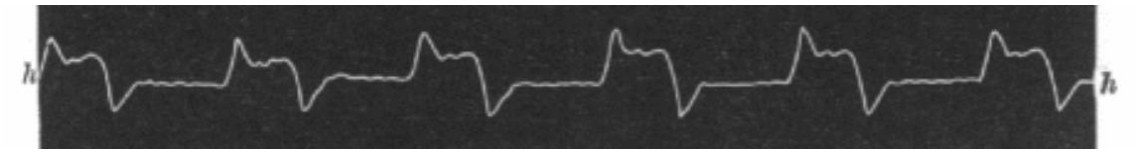

***Figure 7:*** *A cardiograph [38].*

However, Waller was initially not convinced that this new technique would have any extensive use in the hospital [39]. It was another medical doctor and physiologist, Willem Einthoven, who designed a string galvanometer in 1901 – 1903, and was the first able to measure the ECG, comparable to those observed today [40, 41]. He won the Nobel Prize "for his discovery of the mechanism of the ECG" in 1924 [40]. Einthoven is also the one, who named waves of the ECG to be PQRST [42].

The lead is a potential difference between two recording electrodes on the body. Einthoven introduced the use of 3-lead-system for the ECG measurement [43]. Today it is known as Einthoven´s triangle, where leads I, II, and III are known as bipolar limb leads. Later, three augmented unipolar limb leads (aVR, aVL, aVF) and six chest leads (V1 – V6) were added to the tree original ones, and the standard 12-lead electrocardiography was constructed. [33, 34]

The exact wave form in the ECG depends on the electrode connections on the skin surface. From this reason, all electrode locations in 12-lead electrocardiography are standardized. Standardization provides a common base to recognize deviations from the normal signal. [33] The same three electrodes of the bipolar and unipolar limb leads are placed to right arm (RA), left arm (LA) and left leg (LL). Figure 8 shows these three as they are placed in the exercise ECG measurement, but in the normal ECG measurement RA, LA, and LL electrodes are placed on wrists and angle. The bipolar limb leads form

the triangle between these three electrodes. The unipolar limb leads are measuring potential between each electrode and central terminal of the three unipolar leads. Aim of these leads is to reduce effect of inhomogeneity of the body. [34] Figure 8 presents also locations of the chest electrodes, which record electrical activity of the heart in the horizontal plane.

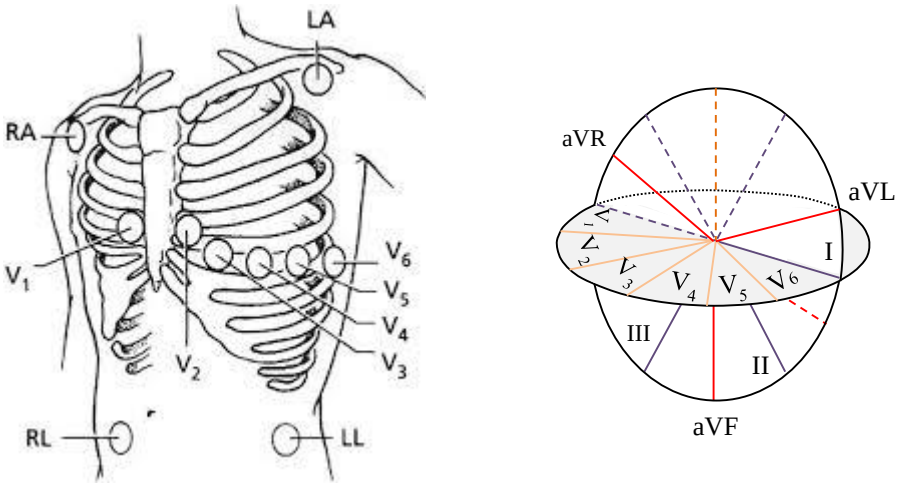


***Figure 8:*** *The 12-lead system [34, 44].*

In addition, there is a one extra electrode placed to the right leg (RL) in Figure 8. Like RA, RL, and LL, in the normal ECG measurement, the RL electrode is placed on the angle instead of the torso. This RL electrode is for a right leg driver (RLD). The RLD is a system for reduce so called common mode voltage from the ECG signal. The common mode voltage is generated by small capacitances between the patient, the power lines and ground. These capacitances cause an interference current of ca. 0.5 micro amperes through the body. When the ECG is measured, the record electrodes are never ideal and cause some impedance of their own. The interference current together with this impedance create undesirable voltage difference between two electrodes. This is seen in the output signal

$$V_{out} = A_d V_d + A_{CM} V_{CM}, \tag{2}$$

where a subscript *d* stands for the amplified (A) differential voltage (V), and a subscript *CM* stands for the undesirable amplified common mode voltage. The RLD senses the common mode voltage through an instrumentation amplifier (INA) and feed the same voltage back to the body. Now the ECG signal is less distorted. [45]

Even though there is a real need for the 12-lead ECG monitoring and for the RLD, mounting and maintaining all ten electrodes is not always possible. Such a large number of electrodes can be inconvenient and impractical for example in emergency monitoring and

long-term monitoring. Increasing number of the ECG channels also affect negatively to signal transmission through telemetry and Internet connections. Alternative choice is to reduce number of leads, as has been done for measurements of this thesis. [46]

### 3.1.2 Diagnostic value of electrocardiography

The ECG is considered as an inexpensive, simple and highly reproducible measurement method. It can be recorded rapidly and equipment is usually always obtainable. In diagnostic testing, the ECG is one of the most commonly performed tests. [47] Already at early days, the ECG was used to observe complete heart block, some arrhythmias, ventricular hypertrophy, extrasystoles and bigeminy. Later it was also used to diagnose the atria related disorders, like atrial fibrillation or atrial flutter. [43]

Today, the principal deviations from the normal ECG can be divided to three categories: (1) abnormalities in rate, (2) abnormalities in rhythm, and (3) cardiac myopathies. Observing the chronology of the atrial and ventricular waves is one of the best ways to analyze arrhythmias in the heart. This is one of the most important applications of the clinical ECG. [34] The information is gathered by studying intervals of the ECG. For example, extension of the P–R interval over 200 milliseconds can indicate damage in the conducting pathways or the AV node. The long Q–T interval time can be due to electrolyte disturbances, conduction problems, coronary ischemia, myocardial damage, or some medications. [35] The S–T interval includes diagnostically interesting S–T segment, which´s depression gives for example information about state of the ischemia of the heart muscle. [48]

Besides of recording the electrical behavior of the heart, the ECG has also potential to reflect anatomy, blood flow, hemodynamics and effect of drugs. [47] Critical diagnostic need of the ECG measurement cannot be denied, because the primary causes of death in Europe are circulatory diseases and the third common causes are heart diseases [49].

## 3.2 Impedance pneumography

The earlies observations about the bioimpedance were made already over 80 years ago (1930s), while the first practical application of respiratory monitoring via bioimpedance was created 30 years later. During 1960s and 70s this type of the respiratory rate (RR) measurement was widely studied, but the interest has been declined since then. [50] Even if the RR has an important role as an indicator in life-threatening situations, it is the most neglected from all vital sign – even for patients with breathing problems. [51–53] This trend is, however, about to be turned. Nowadays, the medical personnel are having more detailed training including the RR. Also changes in devices and methods have effectively increased usage of the RR monitoring. [52, 54]

Bioimpedance is a useful multi-usage tool in the medical applications. It is used for example in impedance cardiography (ICG) and electrical impedance tomography (EIT). Bioimpedance can also provide information about the electrochemical process in the tissue [55]. Bioimpedance spectroscopy (BIS) is a method to study changes of the body composition or fluid balance with multi-frequency techniques. [56, 57] In this thesis, bioimpedance term is referred to the impedance pneumography (IP) measurement. The IP defines changes in electrical conductivity of the thorax caused by breathing, and the RR can be calculated.

### 3.2.1 Respiratory rate

The respiratory rate (RR) describes number of breaths per minute. When the RR is measured, a living tissue is exposed to the small alternating current (AC) from an external source. Different organs resist the current flow in the body. This is known as a bioimpedance. By Ohm´s law, these two elements generate a measurable voltage difference

$$U = ZI, \tag{3}$$

where $Z$ is an impedance, $I$ is an injection current and $U$ is a detected voltage. In Figure 9, the actual voltage signal is presented with light blue. Usually only the filtered signal, presented with dark blue in Figure 9, is shown on the display. The RR can be easily calculated from the filtered and demodulated voltage signal. Increase of the wave presents inhaling and decrease of the wave presents exhaling, so a one peak in the signal corresponds to the one breath. A normal exhaling is happening little faster than an inhaling.

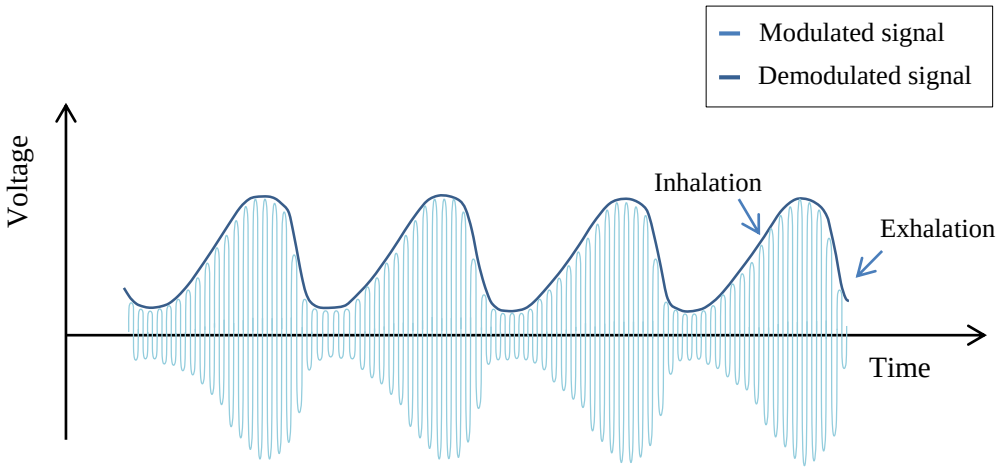


***Figure 9:*** *Detected voltage, when the current injection is a sine wave.*

The impedance pneumography (IP) is an easy, non-invasive way to measure the respiration rate. Even if this measurement does not offer a significant diagnostic value, besides

apnea, it can be used as an indicator of progression of the illness or as a requirement for the immediate clinical attention. [50, 58]

The RR measurement provides valuable information about ventilation during unusual situations like hypoxemia and hypercarbia. They can be recognized from an increase of the tidal volume and the RR. Especially, the hypercarbia is indicating a respiratory failure or conditions like abdominal pathology or sepsis. These can be the best noticed from changes in the RR. [51, 52] The IP monitoring can be life-saving for the post-surgical patients because pain killer opioid drugs can lead to the respiratory depression [59]. It is also observed that serious event, like cardiac arrest, is often preceded by changes in the RR [60]. Further studies have proved the RR to be a critical vital sign while discriminating risk cases from the stable patients [61].

Respiration depends on age, fitness level and stress level. For the adults, a normal breathing rhythm is 12 – 20 breaths per minute. [62] Normally the rate is increased by an illness. Mortality is more likely when the RR is growing at rest [63, 64], as seen in Figure 10.

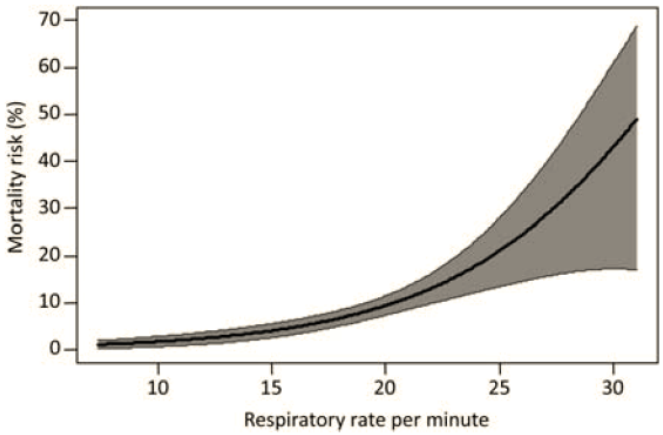


***Figure 10:*** *Effect of the respiratory rate to mortality [64].*

Fieselmann et al. proposed the RR > 27 breaths per minute to be a threshold for physician evaluation [60]. Cretikos et al. observed that the RR > 36 breaths per minute together with other physical factors predict serious event within 24 hours with specificity up to 95.6 % [53]. A year later, the same group success that general ward patients with the RR > 24 breaths per minute should be closely monitored and reviewed regularly, while patients with the RR > 27 breaths per minute should receive immediate medical concern. [51]. On the other hand, it can be too resource consuming to have all patients, with the RR > 24 – 27 breaths per minute, under a special attention. In Fieselmann et al. study, it was estimated that even 17.4 % from all control patients would have exceed the 27 breaths thresh-

old over three day period [60]. Like for many other measurements, specificity and sensitivity are not fully meeting each other when the RR threshold is determined for different cases [53, 60, 65].

### 3.2.2 Measurement settings

The bioimpedance $Z$ can be calculated when the injection current $I$ and a detected voltage $U$ are known. The impedance is composed of two parts: real and imaginary parts.

$$Z = R + jX_C, \tag{4}$$

where $R$ is a resistance caused by a total body water and $X_C$ is a reactance caused by capacitance of the cell membrane. The resistance is depending on a length ($L$), a surface area ($A$), and resistivity of the tissue ($\rho$) [66]:

$$R = \rho \frac{L}{A} \tag{5}$$

The reactance value is affected by an injected signal frequency ($f$) and the capacitance ($C$) of the cell membrane [66]:

$$X_C = \frac{1}{2\pi f C} \tag{6}$$

The current injection into the living tissue is highly regulated. According to EN 60601-1 standard by European Committee for Standardization, the injected ac current cannot be higher than 10 mA [67]. Used frequencies are usually between 5 kHz and 1 MHz. The Cole–Cole model describes simplified cell structure, where $R_e$ is the resistance of an extracellular fluid and $R_i$ is the resistance of an intracellular fluid. $C_m$ is the capacitance of a cell membrane. Current frequency must be high enough to penetrate through this membrane, as seen in Figure 11. [68] Usually the current injection is tens of micro amperes and the frequency is tens of kilo hertz [69–71]. The current injection is so small that it cannot be sensed by the patient.

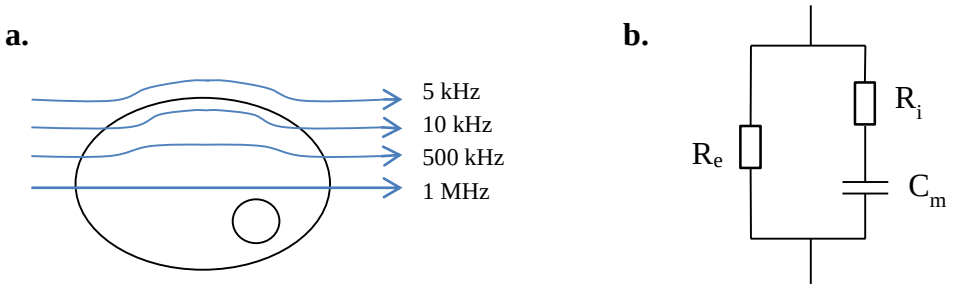


***Figure 11: a.*** *AC frequencies, adapted from [72],* ***b.*** *The Cole-Cole model [68].*

The IP is usually measured with 2- or 4-electrode system. A 2-electrode or bipolar impedance measurement uses its two electrodes for both the current injection and the voltage detection. However, the electrodes and an electrode-tissue-surface cause extra impedance, which is seen as a measurement error in the real body tissue impedance [57]. Electrodes are polarized. In a 4-electrode or tetrapolar impedance measurement, two of the electrodes are for the current injection and another two for the voltage detection. Now impedance of the electrode-tissue-surface is reduced and polarization avoided. Use of the four electrodes also enables observation of the tidal breathing and the respiratory flow measurement, which cannot be achieved in general level with only two electrodes. [73] In addition, advantage of the tetrapolar system lays on sensitivity field S, which can be focused to particular regions, like upper airways, with careful 4-electrode system design. In the bipolar system the sensitivity distribution in the lead field of voltage measurement electrodes $\mathbf{J}_{LE}$ [1/m$^2$] is the same the distribution of the applied current $\mathbf{J}_{LI}$ [1/m$^2$], but in the tetrapolar system the sensitivity distribution is the dot product of the mentioned vectors, as shown in equation 7:

$$Z = \int_v \frac{1}{\sigma} \boldsymbol{S}\, dv = \int_v \frac{1}{\sigma} \boldsymbol{J}_{LE} \bullet \boldsymbol{J}_{LI}\, dv, \tag{7}$$

where v is volume [m$^3$] of the conductor and σ is conductivity [1/Ω · m]. Equation 7 shows measured impedance in certain time *t*. [74] The concept of sensitivity field is shown in Figure 12.

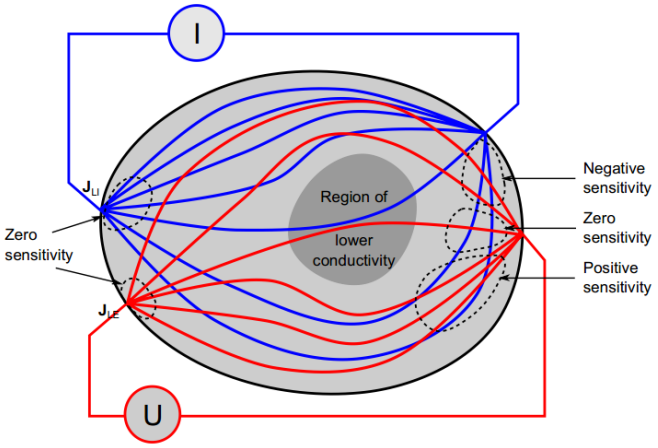


***Figure 12:*** *Sensitivity field of tetrapolar system [50].*

There are three types of sensitivity areas in sensitivity field: positive, zero and negative. In positive sensitivity areas impedance-conductivity relation acts like explained above. In zero sensitivity areas there is no sensitivity or sensitivity is weak. This occur for example in electrodes. The negative sensitivity area changes impedance-conductivity relation in a way where conduction increase also means increase in impedance. [74, 75] This can be seen as a disadvantage when sensitivity field of the tetrapolar measurements may cause error in certain circumstance. It is also said, that tetrapolar measurement is generally more

vulnerable to errors than bipolar system. [76] The electronics companies are also willing to follow rather the bipolar system than the tetrapolar system. Texas Instruments states that the bipolar system is more practical because only two electrodes are needed [77]. This is true, because with four electrodes there is more skin irritation and increasing possibility to lost skin-electrode-contact. Usage of the textile-integrated electrodes degreases skin irritation, but also increases poor skin-electrode-contact compared to disposal electrodes.

It has been studied that placing electrodes in lateral on each side of the thorax is effective way for the IP measurement [75]. In the bipolar system there is only one electrode per side, but for the tetrapolar system there are two vertically placed electrodes per side. In the latter case, a distance between the electrodes should be large enough in order to achieve a good sensitivity field. Locations are presented in Figure 13.

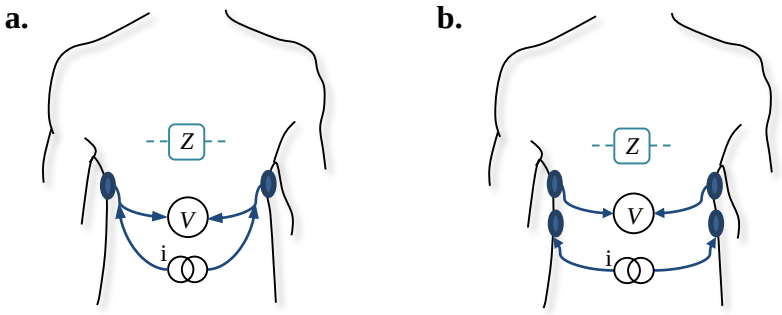


***Figure 13: a.*** *The bipolar, and* ***b.*** *the tetrapolar bioimpedance settings.*

Even if the connection between impedance changes and breathing has been recognized, modelling and origin of the bioimpedance have been controversial. According existing modelling theories, the living tissue can be characterized as an electrolytic conductor or a dielectric biomaterial. In the first model, free ions in intracellular and extracellular liquids are seen as ionic current carriers for direct current (DC) of the skin electrodes. This is reasonable when normal wet (gelled) silver/silver-chloride electrodes are used. However, in case of the dry electrodes, the second model is more suitable. Now there is a galvanic isolation between the skin electrodes, and the tissue between is described as a dielectric. The model can be explained as a capacitor, where body is a dielectric biomaterial between two capacitor plates – in this case, electrodes. [55]

There have been two main theories for the origin of the bioimpedance. According the first theory, changes in the impedance are related to the chest wall movement and thoracic expansion. The alternative theory explains changes of the impedance with lung aeration. Today, source of the IP signal has summarized to be caused by the lung tissue itself.

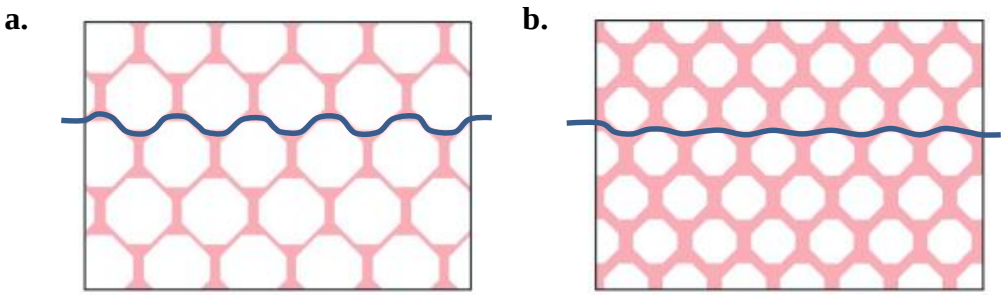


***Figure 14:*** *Conduction path through* ***a.*** *inflated lung and* ***b.*** *deflated lung, adapted from [50].*

When the lungs are filled by air, as seen in Figure 14 a., the lung tissue stretch and its electrical conductivity decreases. When air is exhaled, Figure 14 b., the lung tissue return to the normal state and the electrical conductivity increases. Demonstration of conduction paths is presented in blue. However, the electrode location is affecting how linear the volume-impedance relationship can be. If the electrodes are placed too low, also other than the lung tissue may affect to the signal. Right locations of the electrodes have an important role in volume-impedance linearity. [50]

# 4. MATERIALS AND METHODS

A goal of this thesis was design the textile-integrated ECG and impedance pneumography measurement module in schematic level for the Disappearing sensors (DISSE) project, implemented by Laboratory for Future Electronics, Tampere University of Technology. This chapter presents design process in order to develop an individual measurement module from a half-ready solution.

## 4.1 Application

In Figure 15, block diagram of the total textile-integrated application is presented. It includes sensors, at least two measurement modules, microcontroller and Bluetooth module, battery, and mobile application. The PC program is used to create and control the mobile application. The data is saved to the cloud service.

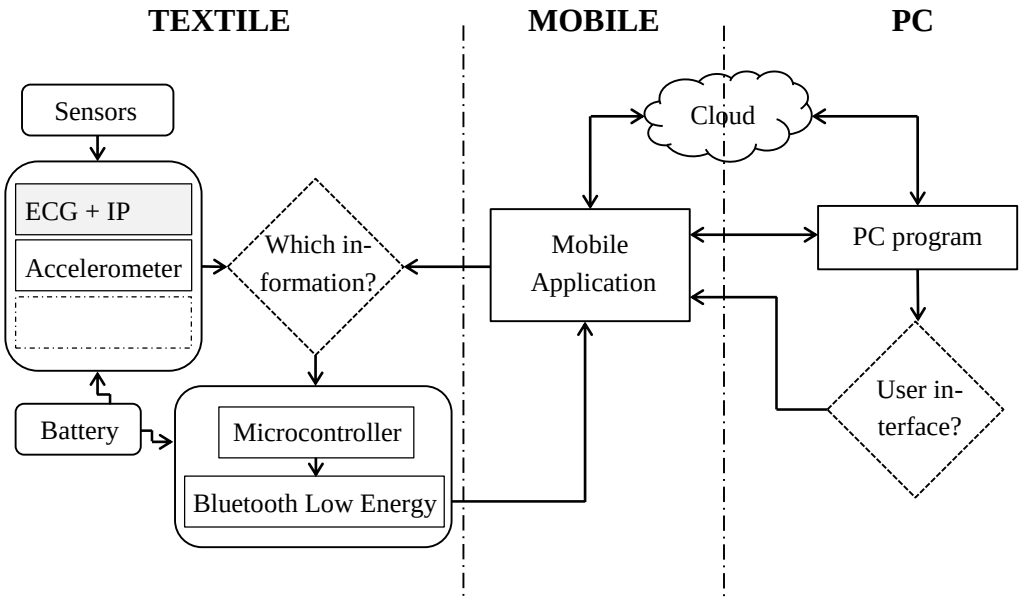


***Figure 15:*** *The application, in which the measurement module is implemented.*

The measurement module, design presented in this thesis, is highlighted with grey. Another measurement module will be the accelerometer. There is also possibility for the third module, which could be for example the temperature measurement module. A data from the selected module is gathered by the microcontroller and transferred to the mobile application through the BLE. The target data transfer frequencies are 500 Hz for ECG signal and 125 Hz for IP signal. Frequency of the ECG signal can be decreased to 250 Hz, if BLE is too limited for higher rates. Also original ADC resolution 24 bits can be

decreased to 16 bits, if needed. The mobile interface for the user is designed on the PC software, Thingworx, which is offered by Elisa.

More specific information about the architecture of the DISSE project is available as "*Development of an Architecture for a Telemedicine Based Longterm Monitoring System*" by Lukas Tietz. "*Methods for Processing and Analyzing Long-Term Physiological Measurements*", by Shadi Mahdiani, clarifies signal processing of the project. Taru Suonurmi studied a measurement module mounting on the textile in "*Component Mounting on Stretchable Substrate*", and "*Printed Stretchable Interconnects for Wearable Health and Wellbeing Applications*", by Jari Suikkola, presents performance and usage of printable wires in detail.

## 4.2 Analog front-end and evaluation board

Possibilities to design light and battery-powered textile-integrated measurement systems have improved in last years. In the 2010s, known electronics companies started to provide precision data converters for the medical applications. [78] These electronics chips are known as medical analog front-ends (AFE). Typically needed components, like instrumentation amplifiers (INA), programmable gain amplifiers (PGA), analog to digital converters (ADC), and filters are built into the small chip, which simplifies and speeds up the design process. The chip can be implemented to the commercial evaluation board, which works as a demonstration platform. The board gives possibility to test functionality of the AFE without having own design around it. Having demonstration saves recourses, because suitability of the AFE for the specific application can easily be observed. For example, the choice of the chip in this thesis was changed due to performance of an evaluation board.

The problem is the AFEs do not provide that much flexibility. It might be challenging to find a suitable chip for the specific design. Another issue is that the selected AFE is likely to include undesired extra properties, which consume energy and hold an extra space. For example, the RLD is not necessarily needed in a minimized ECG AFE.

Finding a suitable medical AFE for the bipolar, and especially, for the tetrapolar ECG and IP measurement, was the first goal in the measurement module design. Main electronics companies nowadays provide medical AFEs for the ECG and other biopotentials, like the electroencephalography and the electromyography. The IP measurement is additional feature for the some AFEs. The most commonly offered AFE is the ECG solution designed for the standard limb leads or for the standard 12-lead ECG, as a combination of the several AFEs [69, 70] or with the one big chip itself [71]. The smallest AFEs measure just a one ECG lead.

Despite of the relatively wide range of the alternatives, requirement of the tetrapolar measurement was main limiting factor. Analog Device´s provides AFEs with a different

number of electrodes, but the ECG and the IP are measured from separated points. [70]. Texas Instruments, on the other hand, has the required AFE but just for the bipolar system [79]. Only the HM301D chip from STMicroelectronics was specifically designed for the desired tetrapolar ECG and IP measurement [69], and it was selected for primary chip choice for this thesis. Besides of the HM301D, STMicroelectronics does not provide any other AFEs, while for example Texas Instruments has even 46 different choices. Lack of the experience is seen in performance of the HM301D. At least functionality of the HM301D´s evaluation board STEVAL-IME002V2 did not met expectations about the succeeded ECG or IP measurements. Because of the arisen issues, the HM301D chip was chosen to be replaced with the secondary choice, the ADS1292R by Texas Instruments. It was noticed that this originally for bipolar measurement designed chip was able to be used, and its evaluation board to be modified, for the tetrapolar measurement as well.

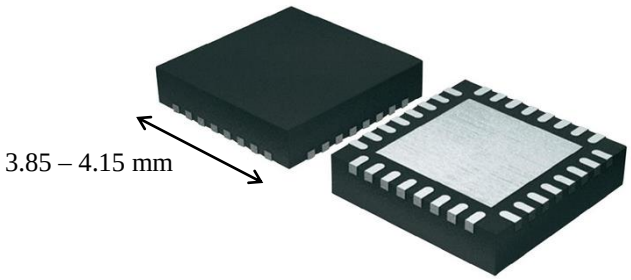


***Figure 16:*** *The model of the ADS1292R in a QFN package [80].*

The ADS1292R, seen in Figure 16, is originally designed for the bipolar ECG and IP measurements, but it can be also used in tetrapolar design. For tetrapolar measurement, the ECG and IP have been measured from the same two electrodes, while another two electrodes are for the current injection. There are two package choices for the ADS1292R: the Quad Flat Package (QFP) and the Quad Flat No-leads package (QFN). Because the module design should be as small as possible, the QFN package, 14.82 – 17.22 $mm^2$, was chosen.

## 4.3 Design of the measurement module

A critical aspect in the medical instrument design is the patient safety. Because this measurement module generates current into the patient, it is important to assure the current to be inside the safety limits. One of the many benefits of the AFE is that it is already programmed to allow only safe current rates and frequencies. For example the ADS1292R is limited to generate the maximum 100 μA current with frequencies from 32 kHz to 64 kHz [71]. Also resistors R1 and R2, seen in appendix A, limit the amount of injected AC current in hardware design. Capacitors C1 and C2, in turn, prevent DC current from being transmitted into the body.

The IP measurement is delicate to errors, because electrodes, wires and measurement device create small amount of extra impedance themselves. In order to minimize this effect, output impedance of the current generator should be as high as possible [57]. Common mode rejection ratio (CMRR) of the device should be high enough to prevent DC current from the measurement signal. In order to improve this value, capacitors C5 and C7 were added to block DC coming from the body. Even though DC protection, some DC may end up to receiver part of the AFE and causes baseline drifting of the ECG [81]. And furthermore, it does not matter if current source and voltage receiver would work identically. There always will be stray capacitance between for example wires and ground, injecting and sensing electrodes, and patient and ground. That is why the injected current cannot be assumed to be exactly the same when it received a tissue – especially with high frequencies.

The schematic was drawn with PADS PCB Design Software by Mentor Graphics. In the design of the measurement module, seen in appendix A, a small size and avoidance of any extra leads were main goals. A small size and light module is more unobtrusive. Number of external connections to the module should be as small as possible. In the final design, there were 32 external components. Printed wires on a textile are critical, because once broken, those cannot be replaced. Number of leads from and to measurement module were minimized, and due this for example the RLD was chosen to be left out from the design. At the end, there was eleven leads for power supply (1), ground (1), serial peripheral interface (SPI) (4), data ready (DRDY) interface (1), and electrode leads (4).

Ensuring that electrodes and leads are properly connected, lead-off detection is used in the design. Recognizing weakness in the electrode-patient connection path is vital for ECG systems, because disturbed signal may not accurately present the monitored ECG. There is two ways to perform lead-off detection: DC and AC methods. DC method is commonly used for lead-off detection in ECG design, because it has minimal impact on the ECG signal. However, if there are failures in conduction path, the excitation signal takes over an original measured input and feed the AFE itself. This is seen as a lead-off event in signal. DC lead-off detection also increases general offset voltage and noise level of the system, as seen in equation 8:

$$V_{offset} = \left[\frac{AVDD-AVSS}{2R_p+R_{in}}\right] R_{in}, \tag{8}$$

where AVDD is voltage of the excitation signal and $R_p$ represents pull-up and pull-down resistors, seen as R3 – R6 in appendix A. $R_{in}$ stands for patient protection electrode, and source impedance. AVSS is potential where excitation signal returns. DC lead-off detection can also be implemented through internal current source or sink. AC lead-off detection is more suitable for dry-contact electrodes, because of capacitive elements of the connectivity path. AC lead-off method monitor the magnitude of an excitation signal fre-

quency to observe lead status. When connection path is disturbed amplitude of the excitation signal is seen at the AFE. If AC lead-off monitoring is chosen, post-processing of the signal in the digital domain is required in order to filter the excitation signal from the ECG. [71, 82]

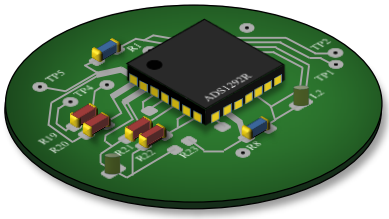

***Figure 17:*** *Example layout design of the measurement module.*

Despite the fact that using a flexible printed circuit board (PCB) would be well suited for textile-integrated application, the rigid alternative provides more support for the electronics [19], and was chosen to be used for the modules in the DISSE project. The layout of the ECG and IP measurement module will be implemented by another member of the project. However, hypothetical layout form of the measurement module is presented in Figure 17.

## 4.4 Bipolar and tetrapolar test methods

The bipolar and tetrapolar measurements methods were tested with evaluation boards from Texas Instruments. Because there are only bipolar evaluation boards available for the ADS1292R, two boards were bought and a one of them was modified for the tetrapolar measurement. In the Figure 18 (b) can be seen how current injection of the second ADS1x9xECG-FE evaluation board is directed to the separated pins of the DB9 port.

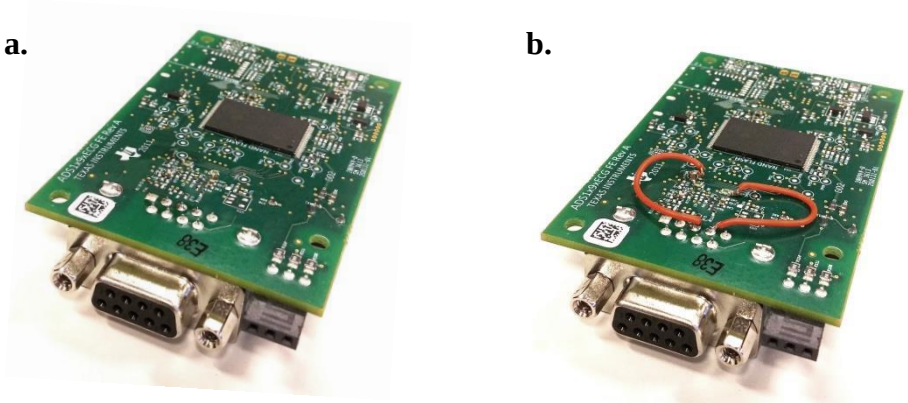


***Figure 18: a.*** *The ADS1x9xECG-FE evaluation board,* ***b.*** *and its modification.*

Modification of the second board is presented in more detail at schematic level in Figure 19. Current injection paths from RESP_MODP and RESP_MODN are reconnected to ELL and ERL instead of original ELA and ERA. In blue is presented new connections to the DB9 port. The red slashes show where previous connections have been broken. The red cross means that this particular component is removed, and crossed do not install (DNI) means that this particular component is installed anyway.

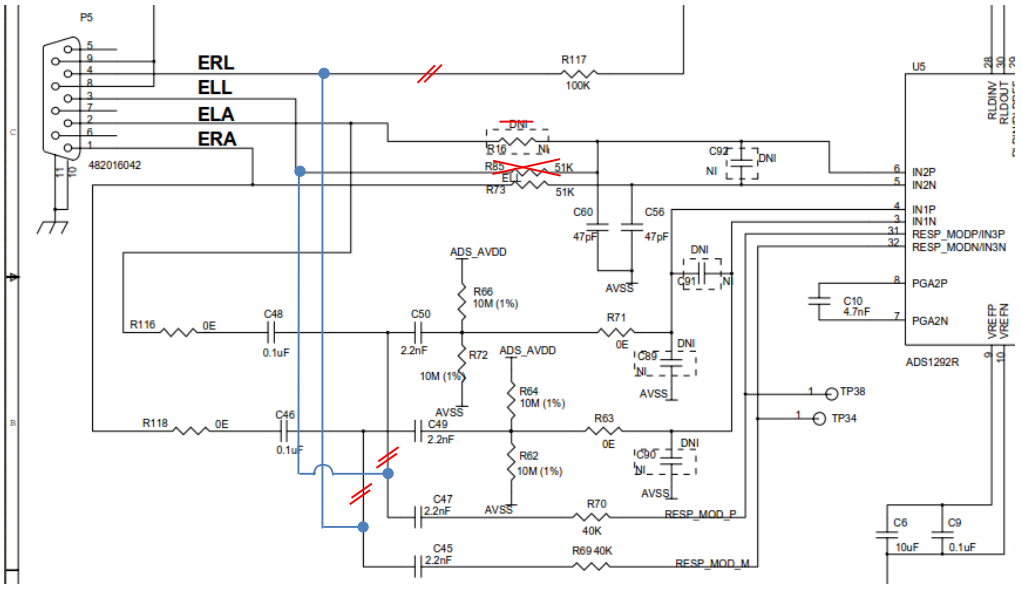


***Figure 19:*** *Modification to second evaluation board in schematic level, adapted from [71].*

In the measurement module design, the current injection can be placed separately, as seen in appendix A, or it can be attached to the measurement electrodes via jumpers. This way both bipolar and tetrapolar measurements are also available with the measurement module.

## 4.5 Measurement plan

There are three variables to be tested: electrodes, measurement position, and measurement techniques. Different electrodes are commercial disposable electrodes, textile electrodes and printed electrodes. The disposable electrodes, Ambu Blue Sensor M-00-S', were used as a reference to compare performance of another two electrodes. Ambu Blue Sensors are gelled wet electrodes, and an example of these electrodes is presented in Figure 20 (a). Sensor area of an electrode is 13.2 $mm^2$. Textile elextrodes, seen in Figure 20 (b) were added on separated elastic textile. Silicon covered multi strand copper wires are connected with 3M electrical tape to the 20x25 mm nylon fabric, which was offered my Clothing+. Dry printable electrodes, seen in Figure 20 (c), were laminated on separated elastic textile. Silicon covered multi strand copper wires are connected to the printed

20x25 mm electrodes via 3M electrical tape. Ink of the printed electrodes is ECM CI-1036. Both the textile and printed electrodes were attached to the T-shirt with Velcro straps.

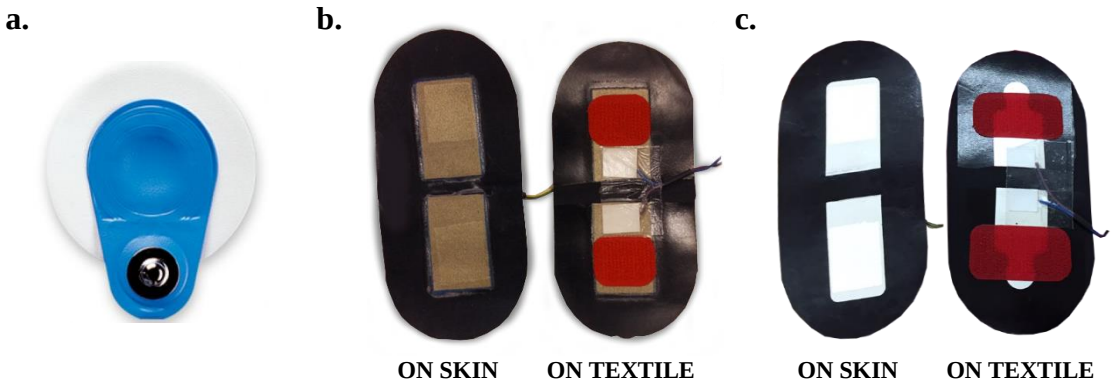


***Figure 20: a.*** *Ambu Blue Sensor [83],* ***b.*** *Textile-electrode,* ***c.*** *Printed electrode*

The Ambu Blue Sensor electrodes were connected through the five output ECG cable from Biopac, seen in Figure 21. Wires of the textile and printed electrodes were connected directly to DB9 port of the evaluations board. In the final prototype all wires were replaced with printed interconnections.

***Figure 21:*** *The ECG cable from Biopack and electrode connectors.*

Each electrode type was tested 5 – 9 times 131 seconds (65500 samples) lasting measurement in sitting, standing and laying positions. There were also two categories for each position: normal breathing and forced breathing. Measurement plan of the forced breathing measurement is presented in Table 1. For each electrode, position and category there

were always at least two different measurement days in order to achieve more comprehensive results.

***Table 1:*** *Phases of the forced breathing measurement.*

| Setting time | Deep breaths | Short breaths | Holding breath | Normal breathing |
|---|---|---|---|---|
| 10 sec | 5 times | 8 times | 15 sec | 31 sec |

The setting time, 10 seconds or 5000 samples, were removed from the beginning of the all measurements. The setting time removal was required, because the user started each measurement herself and was forced to move and touch electrically active devices to do so. This causes errors at the beginning of the measurement. The first 5 recorded cycles represent deep breaths, where a one breath takes 12 seconds (6 + 6 seconds). The next 8 cycles are due fast breathing, where a one breath takes only 2 seconds (1 + 1 seconds). Phase of the short breaths was ended to the eighth inhale, and the lungs were filled by air while holding breath 15 seconds in the next phase. The last section presents uncontrolled normal tidal breathing.

Walking tests were made on a Star Track E-TR treadmill with available speeds 2.5 for the slow and 4.5 for the fast walking. Measurements were repeated 2 – 4 times in normal breathing category and 1 – 3 times in forced breathing category. Walking tests for each electrode type and category there was mainly only one measurement day.

Valuating performance of electrodes was made by visually observing amplitude of noise in signals. In this thesis, this is called a noise ratio of the signal. Average noise ratio for each electrode type in laying, sitting and standing position, and in both breathing categories was determined by calculating average from the three least noisy results separately for the ECG and IP. It must be noted that also the HR and RR detection was made visually while official signal parameter detection program of the DISSE project was still under process when signal analyzes for this thesis were made.

# 5. RESULTS AND DISCUSSION

All the measurement of this thesis were performed on one healthy 25 years old female. Testing was made in random order 2 – 5 hours at a time, between 7:30 am and 9:00 pm, during three months. Measurements were made mainly in one place, but together there were four different measurement locations. Skin was prepared equally for wet and dry electrodes before measurements.

## 5.1 The first prototype

The first prototype of measuring the ECG and IP with ADS1292R and textile-integrated electrodes was constructed from commercial sport T-shirt and bra, evaluation board and handmade electrodes, seen in Figure 20 (b). Electrodes were attached to the T-shirt with Velcro straps. Silicon covered multi strand copper wires from electrodes were brought through holes made into the shirt. The evaluation board was powered by USB-mini input. An output signal was available on PC software offered by Texas Instruments. This simply testing solution is presented in Figure 22.

***Figure 22:*** *The first prototype.*

The shirt is Pro Cool SS Tee sport shirt from Nike. It is made from 84 % polyester and 16 % elastane which ensure fitting shape while the shirt is on. In addition, Victory Compression Bra was attached into the shirt in order to make it more comfortable for female test person to wear. Because of excellent fitting of the shirt and extra support of the sport

bra, sleeves of the shirt did not cause significant extra movement in skin-fabric interface and were allowed to stay in this version.

Based on this first prototype, it can be said there will be at least three major challenges to be solved for upcoming versions. The first problem is going to be maintenance of the shirt. This first version can be washed normally by a machine, because included electronics is removable. However, when electronics is attached permanently to the shirt, a water protection layer must be designed. Several hard parts (modules) of the shirt might also harm surface of a washing machine, so a hand wash might be required anyway. The second problem is related to wearing the shirt. Even though it is only a shirt and bra combination in this first version, there were minor difficulties to put on and take off the shirt. If target group, elderly, is considered, there should be easier way to wear the final prototype in the future. One option is to add a zipper on the back of the shirt while electronics is placed on front. In this way printed connection wires on textile would not either be stretched more than necessary, which would be a case if the shirt is put on traditionally. Horizontal distance between electrodes in first prototype already increases 9 cm when the shirt is worn by the test person. The zipper solution decreases independent usage of a prototype when a subject would need help to wear and remove it. The third problem is going to be how to define different sizes for users. This applies to especially to women, because side of a bra is approximately at the same level with an upper electrode and would prevent required skin-electrode interface. In this first version the problem was avoided by bringing the upper electrodes inside surface of the sport bra instead of the shirt. Still, this cannot be a final solution in non-personalized prototypes, because regular size options for technical shirts and sport bras do not equally match for different body shapes. In Finland, where DISSE project is placed, after age 75 there are more women than men in human population so the problem is quite relevant [84].

An elderly health care experienced nurse, Riina Kujanpää, was interviewed for this thesis about how she would see the future for this kind of measurement shirt. In her opinion, a zipper on back of the shirt would be a good working solution and do not distress a user too much even if an independency is partly lost. Based on her experience, many elder women are willing to wear a bra in daily basics. However, the shirt could still be designed to be used without one. This should significantly ease a wearing process. Now also sizing different options is more simple. A combined technical shirt and sport bra solution, as the prototype is right now, would be challenging to be helped put on with a zipper on it.

## 5.2 Tests with the evaluation board

One of the main goals for this thesis was compare how disposal, textile and printed electrodes perform in this kind of combined IP and ECG measurement. Special interest was in printed electrodes, because those are considered to be used in the final application. Another equally important goal was to determinate if minimum requirement, the RR and HR detection, would be successful during movements in everyday life. In this purpose,

measurements were made in different positions: sitting, standing, laying, and walking slow and fast on a treadmill. In addition, detection of the RR was also tested with forced breathing pattern, seen Figure 23, during different measurements. A DC removing infinite impulse response (IRR) filter, included to the ADS1x9xECG-FE software, is likely the cause for a little amplitude pattern seen in holding breath phase of the signal.

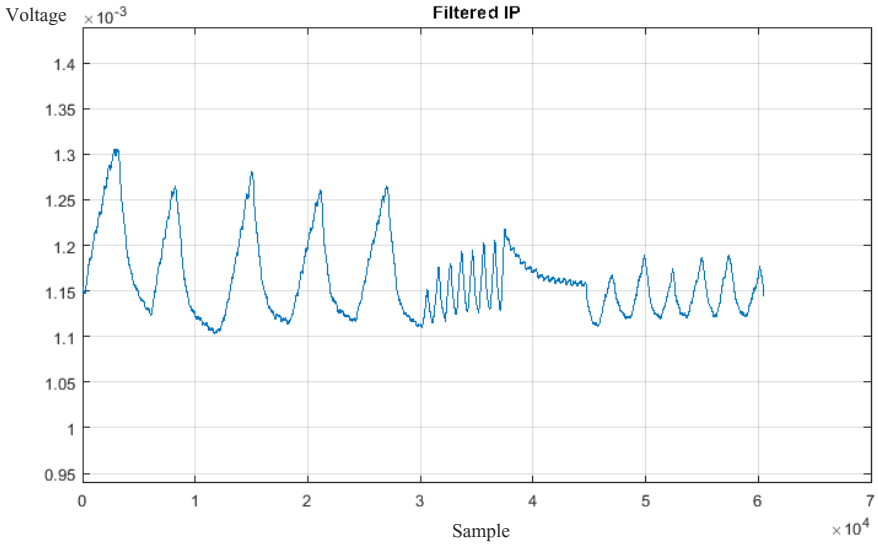


***Figure 23:*** *Forced breathing pattern.*

Electrodes of the bipolar measurement were placed between V and VI rib, and two additional electrodes for the tetrapolar measurement were placed 5,5 cm beneath them, around rib VII. The disposable electrodes were placed in line with the arms while the textile and printed electrodes were placed few centimeters more center in the front side. This is how it was possible to change electrode type in the middle of a measurement for better comparison. The textile and printed electrodes were also likely placed more accurately to the same measurement point, because they are attached into the shirt. When the disposal electrodes were placed by the test person, there was variation in exact locations of electrodes. Also distances between upper and lower electrodes changed between 5 and 5,5 cm, and one side was not necessary equal to another. These differences can cause minor differences between measurements made with disposal electrodes and the textile or printed electrodes.

In Table 2 is presented average noise levels for each electrode type in sitting, standing and laying positions and in both breathing categories and with both measurement techniques. It can be easily pointed out that for the HR measurement, the disposal Ambu electrodes cause the least noise. Between the textile and printed electrodes there are not that much difference. For the RR noise levels there is not clear best electrode type despite the textile electrodes gives evenly good values in tetrapolar measurements. However,

while Ambu and the textile electrodes are good alternatives according noise ratios of the RR measurements, performance of the printed electrodes is not that convincing.

***Table 2:*** *Noise ratios.*

| | | Bipolar | | | Tetrapolar | | |
|---|---|---|---|---|---|---|---|
| RR [µV] | | Ambu | Textile | Printed | Ambu | Textile | Printed |
| Norm | sitting | 61 | 88 | 320 | 224 | 57 | 252 |
| | standing | 50 | 64 | 44 | 88 | 43 | 302 |
| | laying | 65 | 44 | 49 | 57 | 41 | 175 |
| Forced breaths | sitting | 57 | 64 | 343 | 241 | 58 | 430 |
| | standing | 50 | 77 | 287 | 292 | 44 | 220 |
| | laying | 68 | 58 | 49 | 49 | 50 | 112 |
| HR [µV] | | | | | | | |
| Norm | sitting | 950 | 2160 | 1260 | 266 | 2600 | 1810 |
| | standing | 183 | 1230 | 405 | 253 | 1700 | 4360 |
| | laying | 1270 | 1230 | 517 | 148 | 1200 | 927 |
| Forced breaths | sitting | 289 | 1240 | 1470 | 1050 | 2670 | 3350 |
| | standing | 204 | 950 | 917 | 300 | 1860 | 3970 |
| | laying | 1200 | 1970 | 8080 | 198 | 1670 | 1130 |

Forced breathing, in Table 2, cause extra muscle tension in stomach and sides of the body in order to inhale and exhale beyond normal rates. This so called electromyography noise or EMG noise is seen in results, where 72 % from forced breathing measurements are noisier compared to normal breathing measurements. The relation is same for noise levels in the HR measurements.

As expected, a laying position caused less noise compared to sitting and standing positions in most of the measurements, because there is not that much possibility for the EMG noise. At least tetrapolar measurements followed this pattern precisely. In bipolar measurements also standing position gave less noisy values. When noise ratio is low, it is easier to read the ECG signal parameters and gain more information than only the HR.

Detection of the RR and HR was determined visually from filtered data. The IP data was filtered with a low-pass finite impulse response (FIR) filter with order 200 and cutoff frequency at 30 Hz. Also high-pass FIR filter with order 400 and cutoff frequency at 0.002 Hz was applied. The ECG data was filtered with four FIR notch filters with order 200 with stop band between [48,52], [98,102], [148,152] and [198,200] for removing power-line interference at 50 Hz and its harmonics at 100, 150 and 200 Hz. Effect of the listed harmonics is better explained in chapter 5.4. In addition, low-pass FIR filter with order 200 and cutoff frequency at 250 Hz and a high-pass FIR filter with order 400 and cutoff frequency at 0.2 Hz were used to filter the ECG data. In Figure 24 is presented unacceptable examples of a normal and forced breathing. Main reason to a failed normal breathing measurement was too noisy signal to detect individual breathing peaks or signal itself was

too weak and drifted breathing peaks to be separated from each other. Main reason to a failed forced breathing measurement was uncertainty to differ fast breaths phase (samples 4000 – 4800) from breath holding phase (samples 4800 – 5800). Reason for a failed ECG signal was related to errors in signal which could not be filtered and prevented accurate HR detection.

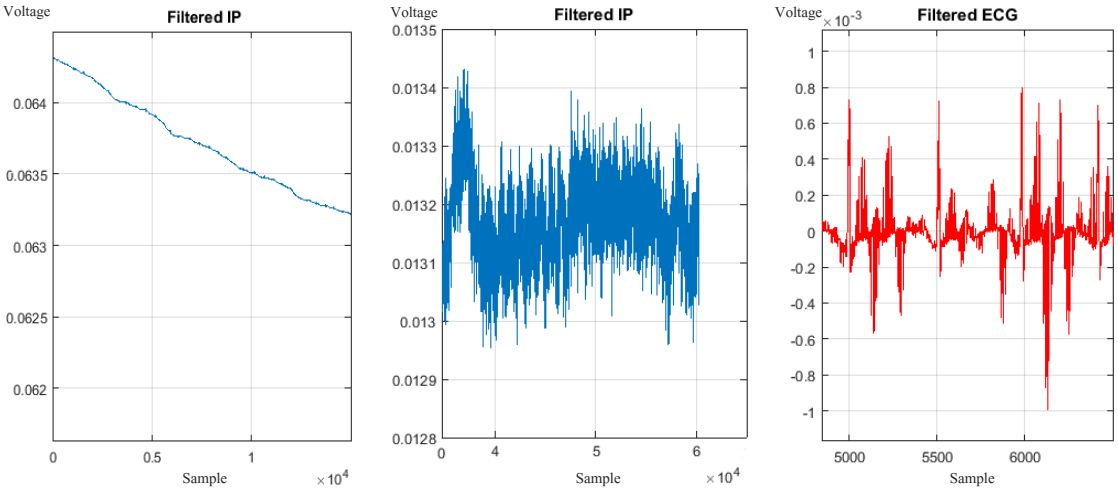


**a.** a weak IP signal **b.** no different in two IP phases **c.** noise peaks in ECG

***Figure 24:*** *Examples of failed results, where the RR or HR could not be detected.*

There was not significant difference between three electrode types to detect the HR. Ambu electrodes were able to display clear R-peaks of the ECG in filtered signal in 96 % accuracy. Both the textile and printed electrodes displayed R-peaks in 98 % accuracy. For the RR detection, breathing peaks were able to be detected with Ambu electrodes in 98 % of cases. For the textile electrodes value was as good as 92 % and for the printed electrodes only 56 %. The RR was generally the noisiest when measured with printed electrodes. In most cases, the RR detection was lost when noise ratio increased over 400 µV. On the other hand, there was not enough data to state in long-term if the textile electrodes truly are the best alternative. Even if measurement for each category were gathered at least from two different days, there were ones for which 4 from 5 measurements were made in one day. This seemed to be a case with tetrapolar printed electrode measurements. One measurement day with poor results did affected to rates. It has to be also noted that using the textile electrodes was otherwise problematic, because there were many cases where a textile electrode measurement was already dismissed before saving to a file due their vulnerability to electrical errors most likely caused by charger of a laptop. The textile electrodes had also unusual effect to the software of evaluation board. In several measurements, the IP signal was reversed without any visible reason. For example, random change in live display settings did recover signal to desired pattern. Problems in performance of the printed electrodes were not that visible, and hence, continued to affect to the test results in later phases.

Even if a sitting, walking excluded, was the noisiest position to measure in general, it was best to detect the HR with 100 % accuracy. While standing detection accuracy of the HR was 95 % and for laying 97 %. The RR was detected with 83 % accuracy in both sitting and standing positions, but only with 73 % accuracy in laying position.

In walking tests, there were two major cause of noise: poor skin-electrode-contact and movement of wires of the electrodes. Also electrode location can cause errors to the signal, because skin stretch and slides slightly at sides of the torso during walking. Disposal Ambu electrodes were the only electrodes which with both the RR and HR could be detected during in most of normal breathing measurements. However, reliable HR detection is easily lost when changing from slow walking to fast walking. It is likely that the reason lays on increasing wire movement, and it can be studied once the first fully textile-integrated prototype is ready. Both with the textile and printed electrodes the RR was detected during normal and forced breathing. Especially difference between fast breaths and holding breath could be more easily be told with these two electrodes rather than with Ambu electrodes. On the other hand, the HR was failed to be detected with either – most likely because worse skin-electrode-connection and less reliable wire connection between the electrodes and the evaluation board. In is presented fast walking test with the bipolar evaluation board and textile electrodes. Due fast walking, now also the RR is hard to detect and the HR is totally lost. Between samples 28 000 and 42 500, the test subject is standing on sides of the treadmill to demonstrate the difference between standing and walking fast positions. This demonstration also excludes the possibility of the treadmill affecting to test results its own.

In Figure 25the future, improvements for skin-electrode-contact must be made in order to improve signals when dry electrodes are used. It can be possible, for example, to add drawstrings to support the contact, even when electrodes are pressed quite firmly against the skin already. Another option is to improve post-signal-processing to filter this kind of signals in more detail.

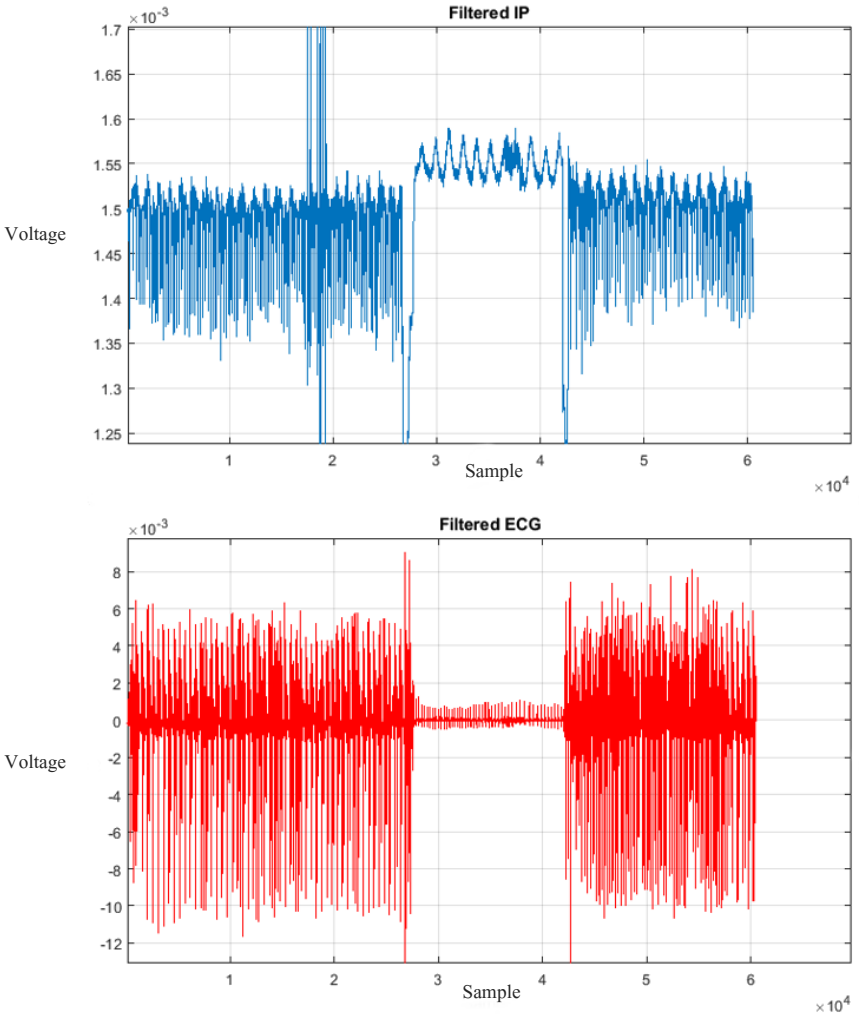


***Figure 25:*** *Differences in signals when walking fast, standing still, and walking fast again.*

Disposable Ambu electrodes were easiest to use, if aspect of the skin irritation is excluded. This is because connection between electrodes and the evaluation board was very certain compared to easily unattached wires of the textile and printed electrodes. When placed, Ambu electrodes stayed exactly in same location during measurements. The printed electrodes had also good and stable connection to the skin in the most measurements. Laminated textile surface around both printed and textile electrodes helped electrodes to stay in one pointed place, because support of the shirt and a natural moisture of the skin prevented laminate surface to move. A surface of the printed electrodes is similar to the laminated textile surface, and seemed to move less against to the skin than the textile electrodes, which have more porous surface. When either the printed or textile electrodes are used, there should be non-conductive extra lamination around them to guarantee better stable connection to the skin.

## 5.3 Bipolar and tetrapolar measurements

For this thesis, alternatives of AFEs for bipolar and tetrapolar ECG and IP measurements were observed. It is clear that manufacturers prefer bipolar measurement method. There was only one tetrapolar IP and ECG measurement AFE designed directly for purposes desired in the DISSE project. However, this HM301D AFE was still under characterization in June 2016, and only engineering samples were available. After testing evaluation board of the HM301D, this AFE was decided to be replaced due a poor performance. The secondary choice was ADS1292R from Texas Instruments, which is designed only for bipolar measurement. Even if Texas Instruments recommend evaluation board of the ADS1292R only be used for bipolar measurements, there was possibility to modify it for tetrapolar measurement as well. Hence, bipolar and tetrapolar measurements was able to be compared as a part of this thesis.

Comparing was made only for sitting, standing, and laying positions. Walking test results were too much affected by wire movements and poor skin-electrode-contact to offer reliable information for this matter.

**Skin irritation**

In Figure 3 (*see Chapter 2.2.*) was presented skin irritation caused by commercial disposal Ambu Blue Sensor electrodes and the printed electrodes. One advantage of the bipolar measurement has been said to be smaller amount of skin irritation due only two electrodes instead of four. However, skin irritation after around 5 hours' use was remarkable only for the disposable electrodes. Because Ambu Blue Sensor M-00-S is intended for short to medium-term applications, removing electrodes this early might cause extra skin irritation itself. Wearing Ambu´s over 12 hours before a remove caused less skin irritation, but marks were still easily seen. In addition, new disposal electrodes could not be attached to the same place at least before one-day period. The printed electrodes did not leave any significant signs on the skin. The textile electrodes did behave similarly to the printed electrodes. It can be said that when the printed or textile electrodes are used, a skin irritation is not valid reason to prefer bipolar measurement over tetrapolar measurement.

**Noise level**

A noise level of measurement signals seemed to be smaller when bipolar method was used. 83 % from the averaged tetrapolar measurements were noisier compared to the bipolar measurement, as seen in Table 3. Presented values are based on the unfiltered data.

***Table 3:*** *Average noise ratio in bipolar and tetrapolar measurements.*

| | Sitting | | | | Standing | | | | Laying | | | |
|---|---|---|---|---|---|---|---|---|---|---|---|---|
| breathing | normal | | forced | | normal | | forced | | normal | | forced | |
| [µV] | RR | HR | RR | HR | RR | HR | RR | HR | RR | HR | RR | HR |
| Bipolar (avg.) | 156 | 1460 | 162 | 2130 | 53 | 606 | 138 | 690 | 66 | 1010 | 58 | 3750 |
| Tetrapolar (avg.) | 176 | 1560 | 243 | 2360 | 144 | 2100 | 185 | 2050 | 91 | 758 | 70 | 999 |

In Figure 26 unfiltered amplitude values of a noise have been presented more comprehensively. From all sitting position measurements, the highest and the lowest noise values were determinate. In addition, average noise level form the best three measurements in each category were calculated. From Table 2, it can be seen that noise ratios of the RR are smaller for the tetrapolar measurement when printed electrodes are used. For disposal and textile electrodes, the bipolar measurement is less noisy. The noise in HR is mainly smaller for all three electrodes in the bipolar measurements. From all average values, only 61 % from tetrapolar measurements is noisier compared to bipolar measurements.

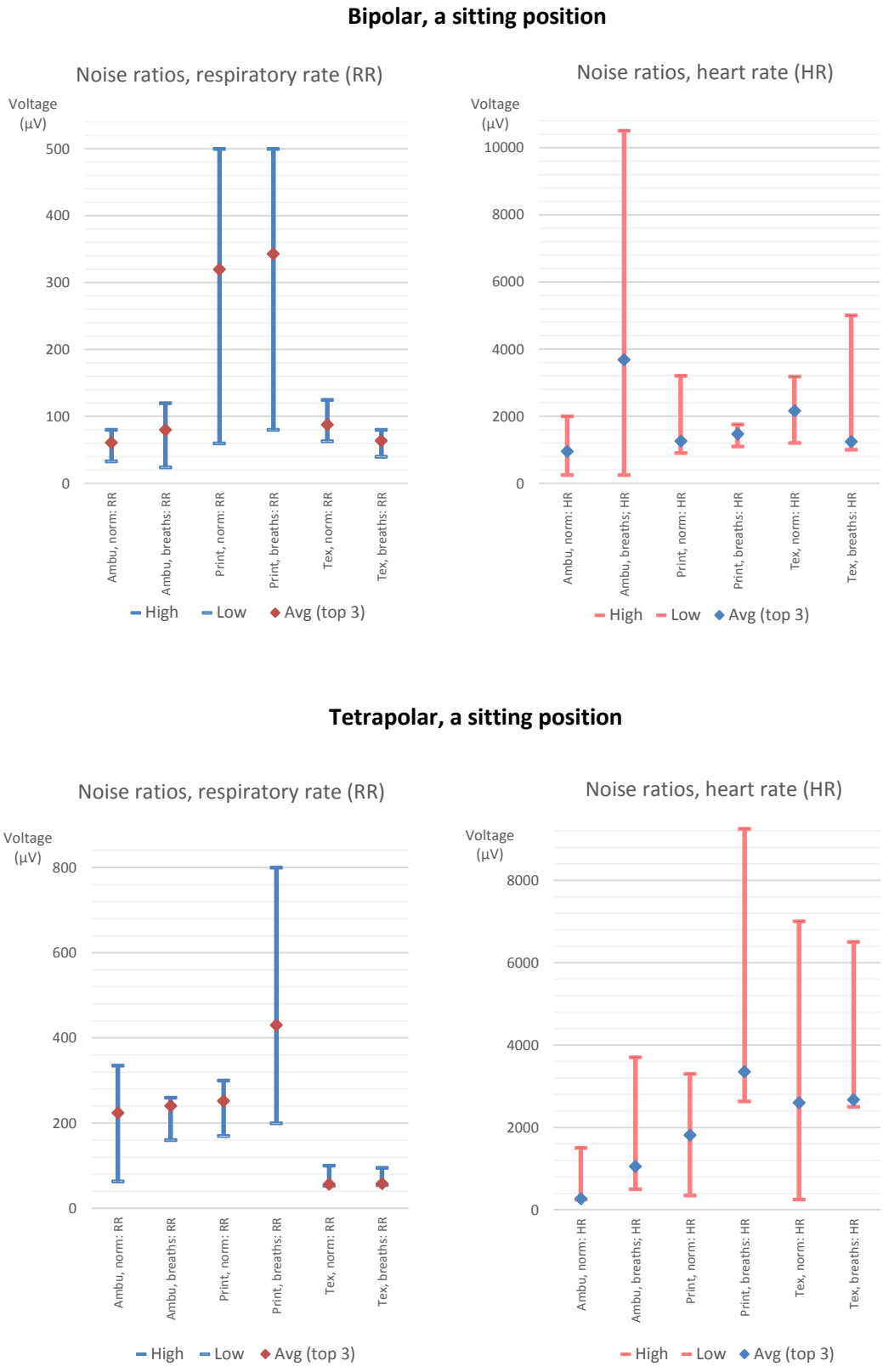


***Figure 26:*** *Variation of noise amplitude in bipolar and tetrapolar measurements.*

In general level, it can be said that usage of the tetrapolar method causes more noise than the bipolar method. This can be partly resulted from only for the bipolar measurements designed AFE and evaluation board. Another cause can be modifications made to the evaluation board in order to change it suitable for the tetrapolar measurement. Noise level of a single measurement, however, does not necessary offer enough information if whether it is made by using the bipolar or tetrapolar method.

Noise level in tetrapolar measurements is more stable compared to bipolar method. In this case, parameters for filtering are easier to define, because a signal does not change. This phenomenon is better explained in the next chapter.

**RR and HR detection**

There were 102 results for the bipolar and 97 results for the tetrapolar measurements. When gathered data was visually observed after a signal filtering process, one was able to justify if the RR and HR could be calculated. From the bipolar measurements results, the RR could be recognized with 76 % and the HR with 97 % accuracy. For the tetrapolar measurements the corresponding values were 82 % for the RR and 99 % for the HR. Based on measurements in this thesis, the tetrapolar method can be considered better to detect the RR and HR, even if it is noisier. With good post-signal-processing the tetrapolar could be better method to be used in the final measurement module.

## 5.4 Factors affecting to the measurement signals

There are several factors which have to be noticed when the IP and ECG signals are observed in this kind of measurement. Otherwise reading the data might lead to wrong conclusions.

**Lead-off detection**

The lead-off detection is very important tool in textile-integrated measurements, because there is a fait chance for electrode not be connected to the skin as planned. The user can fast be informed to check and correct this problem, when a source of the error is known.

Using DC or AC lead-off detection increased noise levels of the IP and ECG signals in the bipolar measurements, excluding Ambu electrodes. However, this behavior was not as clear in the tetrapolar measurements which might be because unfavorable modifications made to the evaluation board. DC lead-off detection was the best alternative to be used when measuring with Ambu electrodes. With filters used for signal processing in this thesis, DC lead-off detection was also better be used with the textile and printed electrodes. With more specifically for the ac lead-off detection signal designed filters the outcome might still be different. Possibility to use the ac lead-off detection for the textile and printed electrodes should be considered again after applying suitable filtering parameters,

but for now it can be said that the DC lead-off detection is sufficient enough for all three electrode types.

Even if there is clear need for lead-off detection and it will be included to the IP and ECG measurement module, it was problematic to use lead-off detection of the software of the ADS1x9xECG-FE evaluation board. There are four lead-off status lights in the software to display if some of the electrodes is not connected properly. It can be said that in almost every measurement IN2N light (for the ECG) did alert from error even when reliable connected Ambu electrodes were in use. Furthermore, the status light did not alert from error when a measurement was acquired, but only in live display mode.

**Forced breathing**

In some measurements, heavy breathing affects to the unfiltered ECG signal itself with noticeable drifting force as seen in a standing position tetrapolar Ambu measurement presented in Figure 27. The effect can be removed in afterward signal processing as made in third case named *Filtered ECG*. However, one can see that even after filtering difference in R-peak sizes remains in the ECG signal.

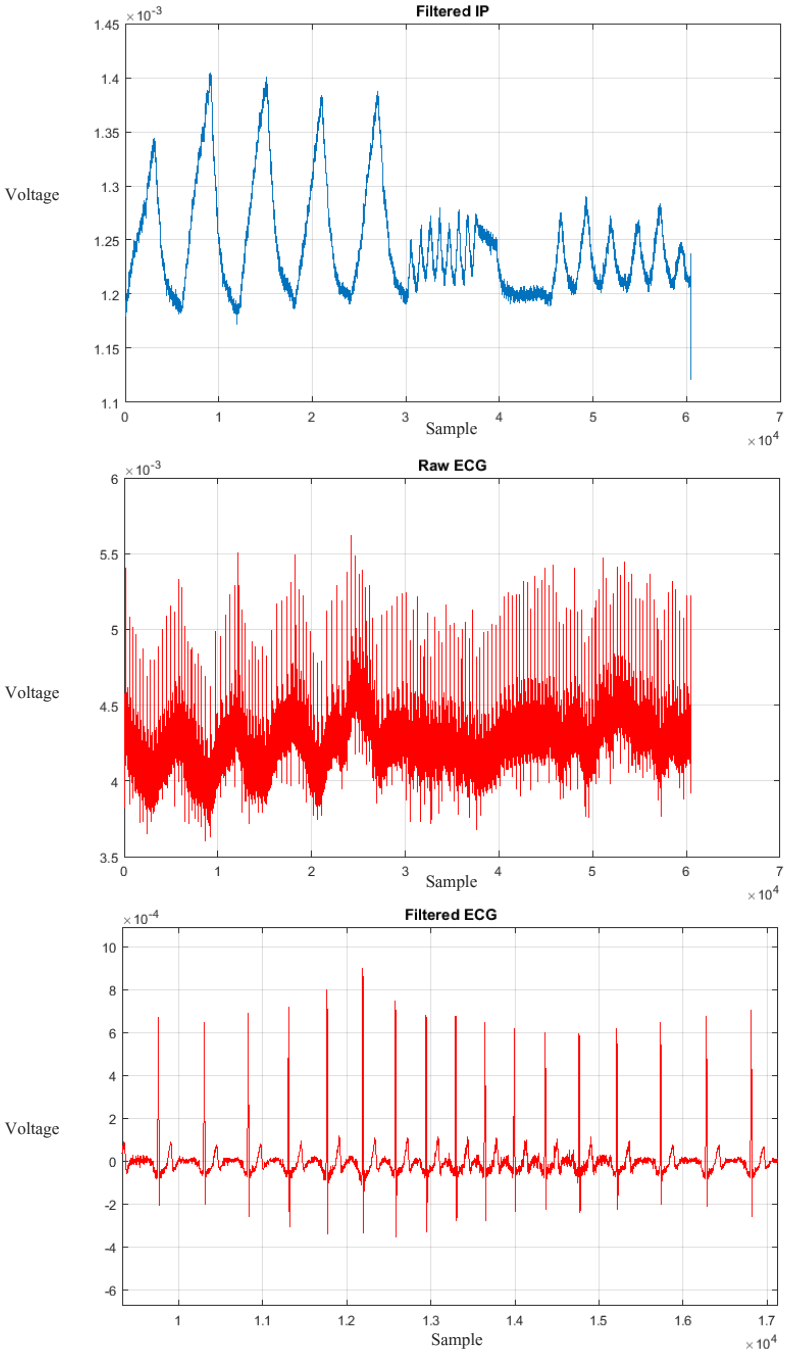


***Figure 27:*** *Forced breathing affecting to the raw ECG signal.*

There are also evidence of a respiratory arrhythmia in the Filtered ECG chart, which means that distance between two R-peaks in the ECG signal is shortened during inspiration and prolonged during expiration.

### Multiplied ECG signal

One significant problem was multiplied noise level in the several, mainly in bipolar measurements occurring, ECG measurements. An example of bipolar printed electrode normal breathing measurement in standing position is shown in Figure 28.

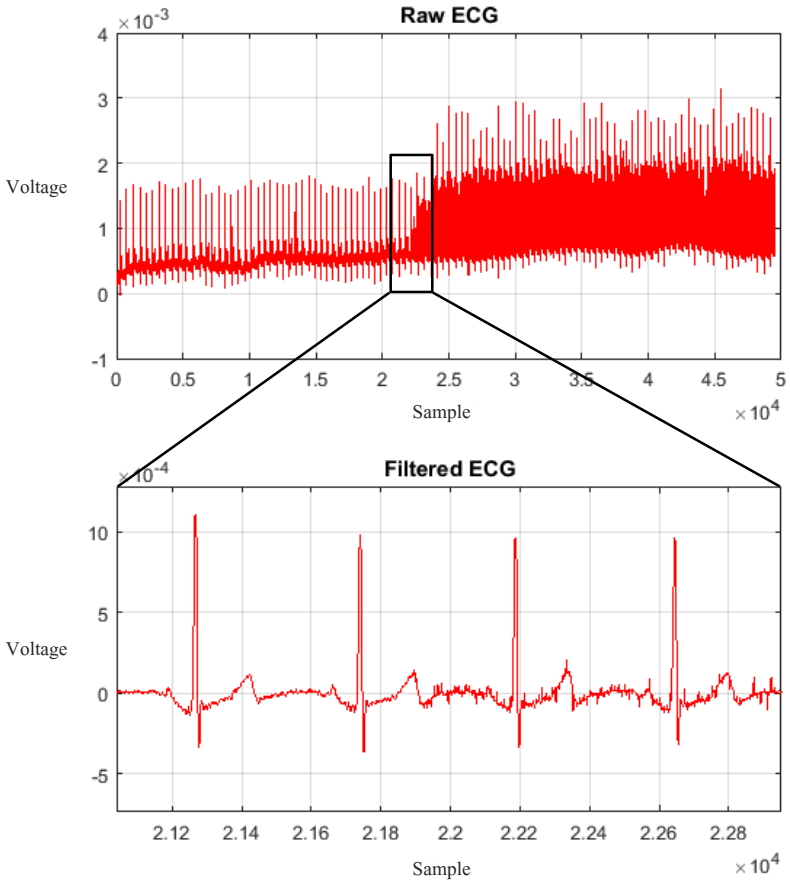


***Figure 28:*** *Noise level multiplying in the ECG signal.*

It was noticed that from some reason in some measurements the power-line interference 50 Hz was harmonized in this case three times to 100, 150 and 200 Hz after around 2200 samples. Even after filtering, the difference between clean and interrupted ECG signals are easily seen, as shown in second chart *Filtered ECG* of the Figure 28.

This unexplained phenomenon recovers to normal state only in few measurements, but that is reason enough to be said that a problem is not necessary in the evaluation board but surroundings. Also Texas Instruments was suggesting that the reason could be for example in fluorescent lights near of a measurement place. However, at the moment the best conclusion is that charger of the used laptop may affect to signal occasionally. When laptop was powered by battery, there was no sign of this phenomenon in the 27 measurement made without charger. When the laptop was not connected to the power-line, the measurement signals were overall less noisy. With this knowledge it can be assumed that

the battery-powered measurement module would offer better IP, and especially, ECG data.

The true effect of the power-line interference is seen while the test person is holding for example a mobile phone, which in turn is connected to its charger. In Figure 29, the test person is holding charging phone in right hand from samples from around 3500 to 6000.

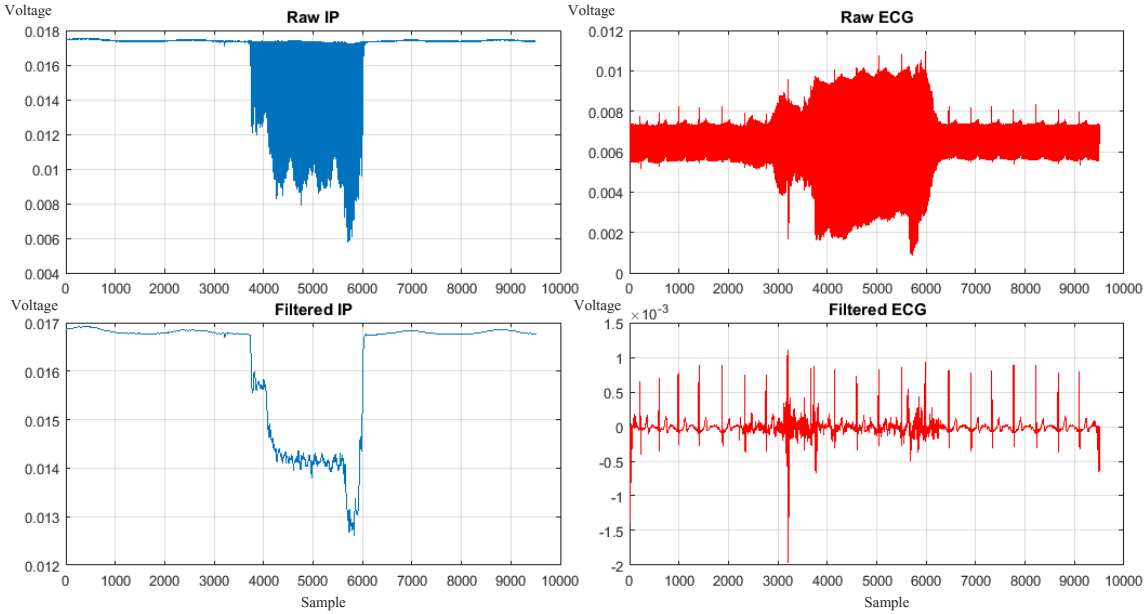


***Figure 29:*** *Power-line interference to the signals through an electrical device.*

Effect this strong is easily seen in both the IP and ECG signals. In addition, the ECG signal is interrupted a little bit earlier because of the EMG noise caused by moving hand to pick a phone. When phone is working on battery there is hardly any visible error in signals, but in live display of the software a small error can be seen also in this case. According to these discovers, the future users should be advised to avoid handling electrical devised connected to the power-line while using the measurement shirt. Also medical personnel viewing the data should be informed about a cause of this kind of error in signals.

# 6. CONCLUSIONS AND FUTURE WORK

In this thesis was made a design for the combined bipolar and tetrapolar techniques including IP and ECG measurement module. Implementation was made with medical analog front-end, ADS1292R, by Texas Instruments. For demo of the upcoming module, the evaluation board ADS1x9xECG-FE was used in order to study difference between bipolar and tetrapolar techniques; which of the three electrode alternatives would work best in this kind of application; and if the RR and HR can be detected during every day activities.

It was learnt that ADS1292R and its evaluation board were able to be used for the tetrapolar measurement even if Texas Instruments recommended those only for their original purposes to be used only for bipolar measurements. In fact, detected the RR and HR were better detected from the tetrapolar measurements than bipolar measurements. However, the tetrapolar measurement included more noise, and may not offer the ECG signal clear enough for diagnostics purposes. Despite this disadvantage, the tetrapolar measurement module not only fulfill the minimum goal but also offer more alternatives of the ways to be used, as explained in this thesis. If in the future, better and more specific post-signal-processing can be developed, the tetrapolar method may be the best measurement technique alternative for the final ECG and IP measurement module.

From electrodes, disposal Ambu electrodes were most reliable, stable, and gave good test results. Because this application is for long-term measurement, the skin irritation caused by Ambu electrodes was intolerable. Despite fact that results for performance of the textile electrodes were generally even better than for Ambu electrodes, there was occasional serious performance problems in them. The textile electrodes could not be trusted to work as desired in all times, as the printed, and especially, the Ambu electrodes did. After overall view, the printed electrodes were considered the most suitable from presented three alternatives for this application, because they did not cause skin irritation in use and mainly achieved the minimum goal in satisfaction. This decision, however, requires that skin-electrode-contact should be improved in order to also maintain minimum goal better during movements. In addition, the lead-off detection have to be observed more deeply in software application of the up-coming module.

Whit the evaluation board it was able to be tested if the minimum goal was achieved during daily activities. Testing positions were laying, sitting, standing and walking slow and fast. It was noticed, like expected, that laying down was best way to achieve a good ECG signal while the IP signal was only acceptable. In general, both the RR and HR were able be detected in all positions excluding walking.

After observing the results, it can be said that this design is workable enough and ready for the next steps for developing a physical form for the module and to integrate it into the textile. With future shirt design and more specific post-signal-processing also performance of the chosen printed electrodes may be improved and at least minimum goal could be achieved during all daily activities.

# 7. REFERENCES

[1] Chronic Conditions: A challenge for the 21st century, (1999). National Academy on an Aging Society, Vol. 1.

[2] Määttänen, A. LähiTapiolan Arjen katsaus: Älyteknologiasta ratkaisu iäkkäiden yksinasumisen tukemiseen - 61 prosenttia suomalaisista suostuisi ikäihmisinä ja yksinasuvina seurattaviksi, web page. Available (accessed 04/04): http://www.lahitapiola.fi/tietoa-lahitapiolasta/medialle/uutiset-ja-tiedotteet/uutiset-ja-tiedotteet/uutinen/1310387597159.

[3] Welch, M. (2014). Biometrics on mobile and wearable devices set to become the universal personal authenticator, Goode Intelligence, United Kingdom.

[4] Nosta, J. Google Glass Meets Prescription Lenses - Something Every Geek Will Love, web page. Available (accessed 03/22): http://www.forbes.com/sites/johnnosta/2014/01/05/google-glass-meets-prescription-lenses-something-every-geek-will-love/#6598b76d2739.

[5] Young, M. Swarovski USB Heart Necklace is a Fashionable Hi-Tech Gadget, web page. Available (accessed 03/22): http://www.trendhunter.com/trends/swarovski-usb-heart-necklace.

[6] Rusty Wired Hoodie, web page. Available (accessed 03/22): http://fashionlab.3ds.com/collection-wired-de-rusty/.

[7] Jawbone UP3, web page. Available (accessed 03/22): http://www.egosmart.eu/en/jawbone-up3-smartwatch.html.

[8] Nike Hyperdunk+ Sport Pack Basketball, web page. Available (accessed 03/22): http://www.lesitedelasneaker.com/2012/06/nike-hyperdunk-sport-pack-basketball/.

[9] RECCO, Advanced Rescue Technology, web page. Available (accessed 02/19): http://www.recco.com/about.

[10] Nathan Sports - LightSpur, web page. Available (accessed 02/19): http://www.nathansports.com/visibility/led-lights/lightspur.

[11] Tile - Never Lose Your Keys, Wallet or Anything again, web page. Available (accessed 02/19): https://www.thetileapp.com/.

[12] Vivago CARE, web page. Available (accessed 02/22): http://www.vivago.fi/tuotteet-ja-palvelut/tuotteet/care-8001/.

[13] Teknologiasta ikääntyneiden arkea: implantit ja etämonitorointi yleistyvät tulevaisuudessa, (2015). Health Operator.

[14] Howard, A. (1998). Hearing Aids: Smaller and Smarter, The New York Times, Vol. November 26.

[15] FDA Approves the First Totally Implanted Hearing System, web page. Available (accessed 02/22): http://www.fda.gov/NewsEvents/Newsroom/PressAnnouncements/ucm204956.htm.

[16] Sensimed Triggerfish, web page. Available (accessed 02/23): http://www.sensimed.ch/en/sensimed-triggerfish/sensimed-triggerfish.html.

[17] Paavilainen, P. (2007). Ikääntyneet teknologian käyttäjinä, Tampere University, School of Health Sciences.

[18] Suikkola, J. (2015). Printed stretchable interconnects for wearable health and wellbeing applications, Tampere University of Technology.

[19] Schlebusch, T., Röthlingshöfer, L., Saim, K., Köny, M. & Leonhardt, S. (2010). On the road to a textile integrated bioimpedance early warning system for lung edema, pp. 302.

[20] Morrison, T., Silver, J. & Otis, B. (2014). A single-chip encrypted wireless 12-lead ECG smart shirt for continuous health monitoring, pp. 1.

[21] Seoane, F., Mohino-Herranz, I., Ferreira, J., Alvarez, L., Buendia, R., Ayllón, D., Llerena, C. & Gil-Pita, R. (2014). Wearable Biomedical Measurement Systems for Assesment of Mental Stress of Combatants in Real Time, Sensors, Vol. 14(4), pp. 7129.

[22] Teichmann, D., Kuhn, A., Leonhardt, S. & Walter, M. (2014). The MAIN Shirt: A Textile-Integrated Magnetic Induction Sensor Array, Sensors, Vol. 14(1), pp. 1039.

[23] Reebok - Checklight, web page. Available (accessed 02/29): http://www.reebok.com/us/checklight/Z85846.html.

[24] Myontec, web page. Available (accessed 02/29): http://www.myontec.com/en/.

[25] OM Smart Shirt, web page. Available (accessed 02/29): http://www.omsignal.com/pages/how-it-works.

[26] Suunto Movesense, web page. Available (accessed 02/24): http://www.suunto.com/Support/Movesense1/Movesense/.

[27] WE:EX - Wearable Experiments: Fox Alert Shirt, web page. Available (accessed 02/29): http://wearableexperiments.com/alert-shirt/.

[28] Prof. Jari Viik (2016). Interview.

[29] Marengoni, A., Winblad, B., Karp, A. & Fratiglioni, L. (2008). Prevalence of the Chronic Diseases and Multimorbidity Among the Elderly Population in Sweden, Am J Public Health, Vol. 98(7), pp. 1198.

[30] Naughton, C., Bennett, K. & Feely, J. (2006). Prevalence of chronic disease in the elderly based on a national pharmacy claims database, Age Ageing, Vol. 35(6), pp. 633.

[31] van den Bussche, H., Koller, D., Kolonko, T., Hansen, H., Wegscheider, K., Glaeske, G., von Leitner, E., Schäfer, I. & Schön, G. (2011). Which chronic disease and disease combinations are specific to multimorbidity in the elderly? Results of a claims data based cross-sectional study in Germany, BMC Public Health.

[32] Ward, B.W., Schiller, J.S. & Goodman, R.A. (2014). Multiple Chronic Conditions Among US Adults: A 2012 Update, Centers for Disease Control and Prevention.

[33] Sherwood, L. (2004). Human Physiology From Cells to Systems, 5th ed., Brooks/Cole, a division of Thomson Learning, USA.

[34] Heikkilä, J., Huikuri, H., Luomanmäki, K., Nieminen, M. & Peuhkurinen, K. (2000). Kardiologia, 1st ed., Kustannus Oy Duodecim, Helsinki.

[35] Martini, F. & Nath, J. (ed.). 2009. Fundamentals of Anatomy & Physiology. 8th ed. United States of America, Pearson Benjamin Cummings.

[36] University of Rochester Medical Center: Anatomy and Function of the System, web page. Available (accessed 03/03): https://www.urmc.rochester.edu/Encyclopedia/Content.aspx?ContentTypeID=90&ContentID=P01762.

[37] Waller, A.D. (1887). On the Electromotive Changes connected with the Beat of the Mammalian Heart, and of the Human Heart in particular, Philosophical Transactions of the Royal Society B, pp. 215.

[38] Waller, A.D. (1887). A Demonstration on Man of Electromotive Changes accompanying the Heart´s Beat, Journal of Physiology, Vol. 8(5), pp. 229.

[39] Quinn, T. (2006). Cardiac Care: An Introduction for Healthcare Professionals - 2. The history of cardiac care, John Wiley & Sons Ltd, England.

[40] Rivera-Ruiz, M., Cajavilca, C. & Varon, J. (2008). Einthoven´s String Galvanometer - The First Electrocardiograph, Texas Heart Institute, Vol. 35(2), pp. 174.

[41] Barr, R.C. (1984). Physiology and Pathophysiology of the Heart - 7. The Electrocardiogram and Its Relationship to Excitation of the Heart, Martinus Nijhoff Publishing, Boston.

[42] Hurst, J.W. (1998). Naming of the Waves in the ECG, With a Brief Account of Their Genesis, Circulation, Vol. 98, pp. 1937.

[43] Barold, S.S. (2003). Willem Einthoven and the Birth of Clinical Electrocardiography a Hundred Years Ago, Cardiac Electrophysiology Review, Vol. 7, pp. 99.

[44] Drew, B., Califf, R., Kaufman, E., Krucoff, M., Laks, M., Macfarlane, P., Sommargren, C., Swiryn, S. & Van Hare, G. (2004). Practice Standards for Electrocardiographic Monitoring in Hospital Settings, Circulation, Vol. 110, pp. 2721.

[45] Metting Van Rijn, A.C., Peper, A. & Grimbergen, C.A. (1990). High-quality recording of bioelectric events. Part 1. Interference reduction, theory and practice, Medical & Biological Engineering & Computing, Vol. 28(5), pp. 389.

[46] Wei, D. (2004). Advances in Electrocardiology - Twelve-Lead Electrocardiogram Telemonitoring, World Scientific Publishing Co. Pte. Ltd., Singapore.

[47] Fish, C. (1989). Evolution of the Clinical Electrocardiogram, JACC, Vol. 14(5), pp. 1127.

[48] Mäkijärvi, M., Kettunen, R., Kivelä, A., Parikka, H. & Yli- Mäyry, S. (ed.). 2011. Sydänsairaudet. 2nd ed. Hämeenlinna, Kariston Kirjapaino Oy.

[49] Eurostats Kuolemansyytilastot, web page. Available (accessed 03/23): http://ec.europa.eu/eurostat/statistics-explained/index.php/Causes_of_death_statistics/fi.

[50] Seppä, V. (2014). Development and Clinical Application of Impedance Pneumography Technique, Doctoral dissertation, Tampere University of Technology.

[51] Cretikos, M.A., Bellomo, R., Hillman, K., Chen, J., Finfer, S. & Flabouris, A. (2008). Respiratory rate: the neglected vital sign, Medical Journal of Australia, Vol. 188(11), pp. 657

[52] Kenward, G., Hodgetts, T. & Castle, N. (2001). Time to put the R back in TPR, Nursing Times, Vol. 97(40), pp. 32.

[53] Cretikos, M., Chen, J., Hillman, K., Bellomo, R., Finfer, S. & Flabouris, A. (2007). The objective medical emergency team activation criteria: A case-control study, Resuscitation, Vol. 73pp. 62

[54] McBride, J., Knight, D., Piper, J. & Smith, G.B. (2005). Long-term effect of introducing an early warning score on respiratory rate charting on general wards, Resuscitation, Vol. 65, pp. 41.

[55] Grimnes, S. & Martinsen, Ø. (2000). Bioimpedance & Bioelectricity Basics, Academic Press, London.

[56] Mialich, M., Sicchieri, J. & Junior, A. (2014). Analysis of Body Composition: A Critical Review of the Use of Bioelectrical Impedance Analysis, International Journal of Clinical Nutrition, Vol. 2(1), pp. 1.

[57] Walker, D. (2001). Modelling The Electrical Properties of Cervical Epithelium, Doctoral dissertation, University of Sheffield.

[58] Kaltiokallio, O., Yigitler, H., Jäntti, R. & Patwari, N. Non-invasive Respiration Rate Monitoring Using a Single COTS TX-RX Pair, IEEE, Vol. 2014: Kaltiokallio, http://elec.aalto.fi/fi/midcom-serveattachmentguidle3cf934502a9eecf9311e3bea02d1b40a9ad7cad7c/p59-kaltiokallio.pdf.

[59] Pattinson, K.T.S. (2008). Opioids and the control of respiration, British Journal of Anaesthesia, Vol. 100(6), pp. 747.

[60] Fieselmann, J., Hendryx, M., Helms, C. & Wakefield, D. (1993). Respiratory rate predicts cardiopulmonary arrest for internal medicine patients, Journal of General Internal Medicine, Vol. 8(7), pp. 354.

[61] AL-Khalid, F.Q., Saatchi, R., Burke, D., Elphick, H. & Tan, S. (2011). Respiration Rate Monitoring Methods: A Review, Pediatric Pulmonology, Vol. 46, pp. 523.

[62] Redmond, C. Trans-thoracic impedance measurements in patient monitoring, web page. Available (accessed 12/15): http://www.edn.com/design/medical/4406838/Trans-thoracic-impedance-measurements-in-patient-monitoring.

[63] Goldhill, D.R., McNarry, A.F., Mandersloot, G. & McGinley, A. (2005). A physiologically-based early warning score for ward patients: the association between score and outcome, Anaesthesia, Vol. 60, pp. 547.

[64] Barthel, P., Wensel, R., Bauer, A., Müller, A., Wolf, P., Ulm, K., Huster, K.M., Francis, D.P., Malik, M. & Schmidt, G. (2012). Respiratory rate predicts outcome after acute myocardial infarction: a prospective cohort study, European Heart Journal.

[65] Rajesh, V.T., Singhi, S. & Kataria, S. (2000). Tachypnoea is a good predictor of hypoxia in acutely ill infants under 2 months, Archives of Diseases in Childhood, Vol. 82, pp. 46.

[66] Khalil, S.F., Mohktar, M.S. & Ibrahim, F. (2014). The Theory and Fundamentals of Bioimpedance Analysis in Clinical Status Monitoring and Diagnosis of Diseases, Sensors, Vol. 14, pp. 10895.

[67] Koivumäki, T. (2014). The Bioimpedance Technique in Respiratory- and Dual-Gated Positron Emission Tomography Imaging, Doctoral dissertation, University of Eastern Finland.

[68] Röthlingshöfer, L., Ulbrich, M., Hahne, S. & Leonhardt, S. (2011). Monitoring Change of Body Fluid during Physical Exercise using Bioimpedance Spectroscopy and Finite Element Simulations, Journal of Electrical Bioimpedance, Vol. 2, pp. 79.

[69] STMicroelectronics, HM301D datasheet, web page. Available (accessed 07/07): http://www.st.com/content/ccc/resource/technical/document/datasheet/99/5f/a5/9b/5c/44/43/68/DM00112265.pdf/files/DM00112265.pdf/jcr:content/translations/en.DM00112265.pdf.

[70] Analog Devices, ADAS1000-3/ADAS1000-4, web page. Available (accessed 07/07): http://www.analog.com/media/en/technical-documentation/data-sheets/ADAS1000-3_1000-4.pdf.

[71] Texas Instruments, ADS129x Low-Power, 8-Channel, 24-Bit Analog Front-End for Biopotential Measurements, web page. Available (accessed 07/07): http://www.ti.com/lit/ds/symlink/ads1294.pdf.

[72] The "Skin Effect" And Bio-Electrical Impedance Analysis, web page. Available (accessed 04/18): http://www.rifevideos.com/the_skin_effect_and_bio_electrical_impedance_analysis.html.

[73] Seppä, V., Uitto, M. & Viik, J. (2013). Tidal Breathing Flow-Volume Curves with Impedance Pneumography During Expiratory Loading, IEEE, pp. 2437.

[74] Malmivuo, J. & Plonsey, R. (1995). Bioelectromagnetism, Oxford University Press, New York.

[75] Seppä, V., Viik, J. & Hyttinen, J. (2010). Assessment of Pulmonary Flow Using Impedance Pneumography, IEEE, Vol. 57(9), pp. 2277.

[76] Grimnes, S. & Martisen, Ø. (2007). Sources of error in tetrapolar impedance measurements on biomaterials and other ionic conductors, Journal of Physics, Vol. 40, pp. 9.

[77] Gupta, A.K. (2011). Respiration Rate Measurement Based on Impedance Pneumography, SBAA181, Texas Instruments.

[78] Partanen, P. (2011). Sydänfilmissä kaiken aikaa, TEK verkkolehti.

[79] Texas Instruments, Low-Power, 2-Channel, 24-Bit Analog Front-End for Biopotential Measurements, web page. Available (accessed 07/07): https://upverter.com/datasheet/f39f35c56d2f15248d62f0eb022e7b7680d7e31f.pdf.

[80] Digi-Key Electronics Xilinx Inc. XC2C32A-6QFG32C, web page. Available (accessed 04/19): http://www.digikey.com/product-detail/en/xilinx-inc/XC2C32A-6QFG32C/122-1412-ND/966593.

[81] Suh, S.C., Gurupur, V.P. & Tanik, M.M. (ed.). 2011. Biomedical Engineering: Health Care Systems, Technology and Techniques. 1st ed. USA, Springer Science+Business Media.

[82] Anthony, C. (2012). Understanding Lead-Off Detection in ECG, SBAA196A, Texas Instruments, USA.

[83] Medkit Ambu Blue Sensor M-OO-S-elektrodi, web page. Available (accessed 04/14): http://www.medkit.fi/ambu-blue-sensor-m-oo-s.

[84] Findikaattori, Väestön ikärakenne, web page. Available (accessed 07/07): http://www.findikaattori.fi/fi/14.

# APPENDIX A: ADS1292R CIRCUIT SHEMATIC